Table 1. Chemical profiles of UCP3 transgenic mice on standard chow and high-fat diets

	Standard chow diet		High-fat diet	
	UCP3 transgenic mice	Non-transgenic littermates	UCP3 transgenic mice	Non-transgenic littermates
Glucose (mmol/l)				
Fasting	6.4±0.2	6.8±0.4	8.9±0.4	10.3±1.1
Non-fasting	8.2±0.6	8.4±0.6	9.9±1.2	11.3±0.9
Insulin (pmol/l)				
Fasting	44±10	48±17	215±32	224±99
Non-fasting	95±20	91±13	638±77	649±170
Cholesterol (mmol/l)	2.15±0.08	2.25±0.10	3.88±0.18	4.22±0.47
Triglyceride (mmol/l)	0.27±0.05	0.36±0.07	0.41±0.05	0.45±0.06
Fatty acids (mmol/l)	1.27±0.14	1.25±0.23	0.83±0.06	0.90±0.07

Data are means ± SE (n=5 to 7)

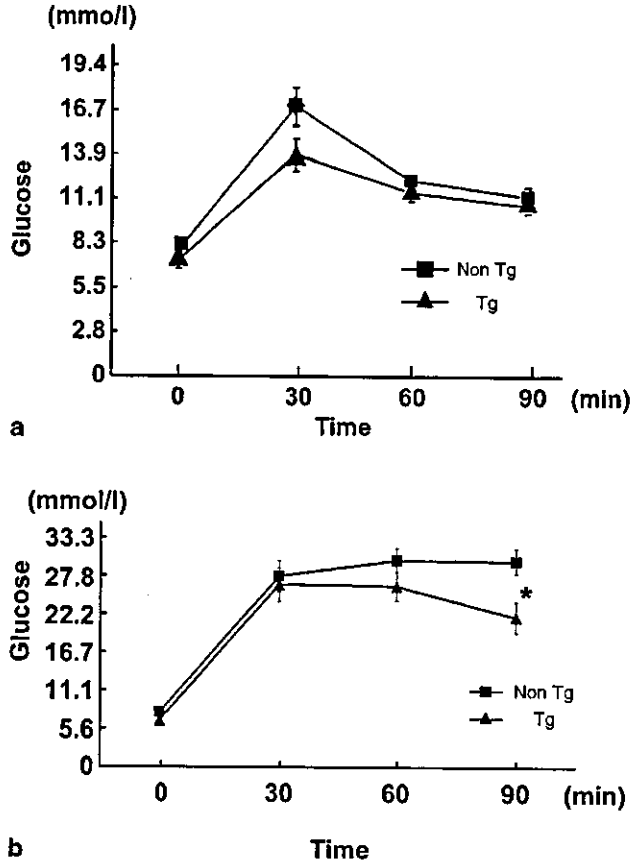

Fig. 5a, b. Glucose tolerance test in (**a**) male 28-week-old transgenic mice and non-transgenic littermates on a standard chow diet and (**b**) in male 28-week-old transgenic mice and non-transgenic littermates after 4 weeks on a high-fat diet. Data are expressed as means ± SE (n=7 to 9). *p<0.05 vs non-transgenic littermates

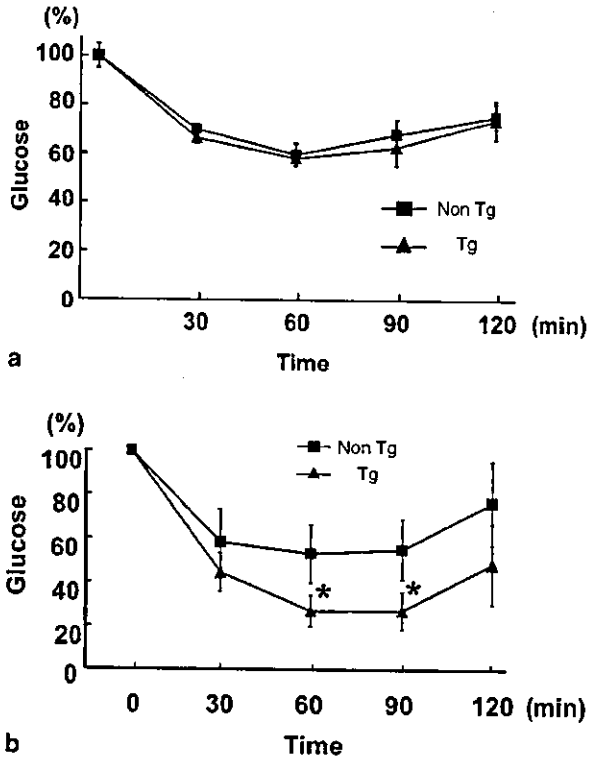

Fig. 6a, b. Insulin tolerance test in (**a**) male 28-week-old transgenic mice and non-transgenic littermates on a standard chow diet and (**b**) in male 28-week-old transgenic mice and non-transgenic littermates after 4 weeks on a high-fat diet. Serum glucose concentrations are expressed as percentages of the initial values of transgenic mice and non-transgenic littermates. Data are expressed as means ± SE (n=7 to 9). *p<0.05 vs non-transgenic littermates

high-fat diet (1693±131 mg vs 2110±17 mg, p<0.05). No difference was observed in the weight of livers or other organs. Histological analyses did not show any obvious difference between transgenic mice and non-transgenic littermates after the 4-week high-fat diet.

Food intake and oxygen consumption of transgenic mice on high-fat diet. No difference in food intake and rectal temperature was noted between transgenic mice and non-transgenic littermates (food intake: 2.5±0.15 g/day vs 2.3±0.08 g/day, p>0.05; rectal tem-

perature: 35.8±0.5°C vs 35.6±0.7°C, $p>0.05$). However, total oxygen consumption for 24 h was higher in transgenic mice than in non-transgenic littermates (54.1±4.5 ml kg^{-1} min^{-1} vs 43.1±1.6 ml kg^{-1} min^{-1}, $p<0.05$).

Blood analysis of transgenic mice on high-fat diet. No significant differences in serum concentrations of glucose, insulin, cholesterol, triglyceride and fatty acids were found between transgenic mice and non-transgenic littermates. However, the relevant values tended to be lower in transgenic mice (Table 1).

Glucose homeostasis in transgenic mice on high-fat diet. In the glucose tolerance test, increases in serum glucose were less marked in transgenic mice than in non-transgenic littermates (n=5 to 7, $p<0.05$; Fig. 5b). In the insulin tolerance test, hypoglycaemic responses 60 and 90 min after the injection were more pronounced in transgenic mice than in non-transgenic littermates (n=5 to 7, $p<0.05$; Fig. 6b).

Discussion

We generated transgenic mice that overexpressed mouse UCP3 in the skeletal muscle by using MCK promoter. In these mice UCP3 overexpression was targeted mainly to the skeletal muscle. Levels of UCP3 mRNA and protein were approximately 18-fold and 15-fold higher in the lines with the highest expression. Northern blot analyses detected a slight increase of UCP3 mRNA in the cardiac muscle. UCP3 mRNA levels in the cardiac muscle of transgenic mice were less than 1% of those in their skeletal muscle. Western blot analyses failed to detect the band of UCP3 in the cardiac muscle in our study. UCP3 mRNA levels in the brown adipose tissue of transgenic mice were not significantly different from those of non-transgenic littermates. No band of UCP3 mRNA was detected in tissues of transgenic mice other than skeletal muscle, cardiac muscle and brown adipose tissue. The phenotype described here therefore results primarily from the expression of the transgene in the skeletal muscle.

Expression of the UCP3 gene has been reported to increase 10- to 20-fold in response to physiological stimuli such as fasting [14]. An approximately 18-fold increase of UCP3 mRNA, as observed in transgenic mice in our study, seems to be feasible by physiological or pharmacological stimuli in vivo.

Our findings for mice on a standard chow diet, with no significant differences across a wide range of factors studied, indicate that an approximately 18-fold overexpression of UCP3 mRNA does not strongly affect energy expenditure on a standard chow diet. However, after a 4-week high-fat diet, transgenic mice were approximately 14% less obese than non-transgenic littermates. This finding is consistent with the tendency of transgenic mice to weigh less on a standard chow diet than their non-transgenic littermates. The increase in body weight of transgenic mice for this 4-week period was nearly 50% less than that of non-transgenic littermates. Moreover, the mean weight of the epididymal fat pad was approximately 20% lower in transgenic mice than in non-transgenic littermates after a 4-week high-fat diet. As no significant difference in food intake was noted between transgenic mice and non-transgenic littermates, the reduction of body weight and epididymal fat pad can be explained by the significantly increased oxygen consumption of transgenic mice on a high-fat diet. The reason why oxygen consumption was significantly increased on a high-fat diet but not on a standard chow diet is not clear. It is also not clear whether the improved glucose tolerance and insulin sensitivity seen in transgenic mice as compared with non-transgenic littermates can be explained by the reduction of obesity or by any other mechanisms.

In one study on transgenic mice which overexpressed human UCP3 mRNA by approximately 66-fold in the skeletal muscle [13] transgenic mice on standard chow were leaner and had decreased adipose tissue mass, improved glucose metabolism and increased metabolic rates (oxygen consumption). The phenotype of transgenic mice on a standard chow diet in this study was consistent with that of our transgenic mice on a high-fat diet. The discrepancy between their and our phenotypes on a standard chow diet could be explained by the difference in mRNA levels of overexpressed UCP3 (66-fold vs 18-fold). Recently the same authors reported that the increase in protein levels of overexpressed UCP3 in their transgenic mice was approximately 23-fold [27], which was also larger than in our transgenic mice (23-fold vs 15-fold). Although this difference in the UCP3 protein levels is not so large, it is possible that a small difference of UCP3 protein concentration in this range is critical for the discrepancy between phenotypes on a standard chow diet. Alternatively, the discrepancy could be due to the difference in the species of overexpressed transgene (human UCP3 vs. mouse UCP3). Taken together with these other findings, our study suggests that overexpression of UCP3 can cause increased energy expenditure, resulting in less adipose-tissue mass and improved glucose metabolism.

In conclusion, our transgenic mice with approximately 18-fold overexpression of UCP3 mRNA did not show any obvious phenotype on a standard chow diet, but were less obese and had improved glucose tolerance on a high-fat diet. As an 18-fold increase of UCP3 mRNA could be attained by physiological or pharmacological stimuli, our results suggest that drugs which increase UCP3 could be effective against obesity and Type 2 diabetes, with few adverse effects.

Acknowledgements. This work was supported in part by research grants from the Japanese Ministry of Education, Culture, Sports, Science and Technology; the Japanese Ministry of Health, Labour and Welfare; Ono Medical Research Foundation; Japan Diabetes Foundation; Tanabe Medical Frontier Conference; and in Canada from the Natural Sciences and Engineering Research Council and the Canadian Institutes of Health Research. We thank Professor S.D. Hauschka for providing p3300MCKCAT, which contains MCK promoter. We also gratefully acknowledge the assistance of Dr S. Monemdjou in the studies of muscle mitochondrial proton leak kinetics, and thank Dr M. Hirode and Dr Y. Sakura for the histological analysis.

References

1. Larkin S, Mull E, Miao W et al. (1997) Regulation of the third member of the uncoupling protein family, UCP3, by cold and thyroid hormone. Biochem Biophys Res Commun 240:222–227
2. Boss O, Samec S, Paoloni-Giacobino A et al. (1997) Uncoupling protein-3: a new member of the mitochondrial carrier family with tissue-specific expression. FEBS Lett 408:39–42
3. Matsuda J, Hosoda K, Itoh H et al. (1997) Cloning of rat uncoupling protein-3 and uncoupling protein-2 cDNAs: their gene expression in rats fed high-fat diet. FEBS Lett 418:200–204
4. Gong DW, He Y, Karas M, Reitman M (1997) Uncoupling protein-3 is a mediator of thermogenesis regulated by thyroid hormone, beta3-adrenergic agonists, and leptin. J Biol Chem 272:24129–24132
5. Zurlo F, Larson K, Bogardus C, Ravussin E (1990) Skeletal muscle metabolism is a major determinant of resting energy expenditure. J Clin Invest 86:1423–1427
6. Klaus S, Casteilla L, Bouillaud F, Ricquier D (1991) The uncoupling protein UCP: a membraneous mitochondrial ion carrier exclusively expressed in brown adipose tissue. Int J Biochem 23:791–801
7. Weigle DS, Selfridge LE, Schwartz MW et al. (1998) Elevated free fatty acids induce uncoupling protein 3 expression in muscle: a potential explanation for the effect of fasting. Diabetes 47:298–302
8. Nagase I, Yoshida T, Saito M (2001) Up-regulation of uncoupling proteins by beta-adrenergic stimulation in L6 myotubes. FEBS Lett 494:175–180
9. Matsuda J, Hosoda K, Itoh H et al. (1998) Increased adipose expression of the uncoupling protein-3 gene by thiazolidinediones in Wistar fatty rats and in cultured adipocytes. Diabetes 47:1809–1814
10. Vidal-Puig AJ, Grujic D, Zhang CY et al. (2000) Energy metabolism in uncoupling protein 3 gene knockout mice. J Biol Chem 275:16258–16266
11. Gong DW, Monemdjou S, Gavrilova O et al. (2000) Lack of obesity and normal response to fasting and thyroid hormone in mice lacking uncoupling protein-3. J Biol Chem 275:16251–16257
12. Huppertz C, Fischer BM, Kim YB et al. (2001) Uncoupling protein 3 (UCP3) stimulates glucose uptake in muscle cells through a phosphoinositide 3-kinase-dependent mechanism. J Biol Chem 276:12520–12529
13. Clapham JC, Arch JR, Chapman H et al. (2000) Mice overexpressing human uncoupling protein-3 in skeletal muscle are hyperphagic and lean. Nature 406:415–418
14. Boss O, Hagen T, Lowell BB (2000) Uncoupling proteins 2 and 3: potential regulators of mitochondrial energy metabolism. Diabetes 49:143–156
15. Son C, Hosoda K, Matsuda J et al. (2001) Up-regulation of uncoupling protein 3 gene expression by fatty acids and agonists for PPARs in L6 myotubes. Endocrinology 142:4189–4194
16. Shintani M, Nishimura H, Akamizu T et al. (1999) Thyrotropin decreases leptin production in rat adipocytes. Metabolism 48:1570–1574
17. Johnson JE, Wold BJ, Hauschka SD (1989) Muscle creatine kinase sequence elements regulating skeletal and cardiac muscle expression in transgenic mice. Mol Cell Biol 9:3393–3399
18. Ogawa Y, Masuzaki H, Hosoda K et al. (1999) Increased glucose metabolism and insulin sensitivity in transgenic skinny mice overexpressing leptin. Diabetes 48:1822–1829
19. Ogawa Y, Masuzaki H, Isse N et al. (1995) Molecular cloning of rat obese cDNA and augmented gene expression in genetically obese Zucker fatty (fa/fa) rats. J Clin Invest 96:1647–1652
20. Sivitz WI, Fink BD, Donohoue PA (1999) Fasting and leptin modulate adipose and muscle uncoupling protein: divergent effects between messenger ribonucleic acid and protein expression. Endocrinology 140:1511–1519
21. Yamamoto Y, Yoshimasa Y, Koh M et al. (2000) Constitutively active mitogen-activated protein kinase kinase increases GLUT1 expression and recruits both GLUT1 and GLUT4 at the cell surface in 3T3-L1 adipocytes. Diabetes 49:332–339
22. Monemdjou S, Kozak LP, Harper ME (1999) Mitochondrial proton leak in brown adipose tissue mitochondria of Ucp1-deficient mice is GDP insensitive. Am J Physiol 276:E1073–E1082
23. Monemdjou S, Hofmann WE, Kozak LP, Harper ME (2000) Increased mitochondrial proton leak in skeletal muscle mitochondria of UCP1-deficient mice. Am J Physiol Endocrinol Metab 279:E941–E946
24. Chen RF (1967) Removal of fatty acids from serum albumin by charcoal treatment. J Biol Chem 242:173–181
25. Ishihara K, Oyaizu S, Onuki K, Lim K, Fushiki T (2000) Chronic (-)-hydroxycitrate administration spares carbohydrate utilization and promotes lipid oxidation during exercise in mice. J Nutr 130:2990–2995
26. Masuzaki H, Ogawa Y, Hosoda K, Kawada T, Fushiki T, Nakao K (1995) Augmented expression of the obese gene in the adipose tissue from rats fed high-fat diet. Biochem Biophys Res Commun 216:355–358
27. Cadenas S, Echtay KS, Harper JA et al. (2002) The basal proton conductance of skeletal muscle mitochondria from transgenic mice overexpressing or lacking uncoupling protein-3. J Biol Chem 277:2773–2778

0021-972X/04/$15.00/0
Printed in U.S.A.

The Journal of Clinical Endocrinology & Metabolism 89(5):2360–2364

doi: 10.1210/jc.2003-031211

Gene and Phenotype Analysis of Congenital Generalized Lipodystrophy in Japanese: A Novel Homozygous Nonsense Mutation in Seipin Gene

KEN EBIHARA, TORU KUSAKABE, HIROAKI MASUZAKI, NOZOMI KOBAYASHI, TOMOHIRO TANAKA, HIDEKI CHUSHO, FUMIKO MIYANAGA, TAKASHI MIYAZAWA, TATSUYA HAYASHI, KIMINORI HOSODA, YOSHIHIRO OGAWA, AND KAZUWA NAKAO

Department of Medicine and Clinical Science, Kyoto University Graduate School of Medicine, Kyoto 606-8507, Japan

Congenital generalized lipodystrophy (CGL), Berardinelli-Seip syndrome, is a rare metabolic disorder characterized by a near total lack of adipose tissue from birth or early infancy. Recently, *seipin*, encoding a 398-amino acid protein of unknown function, and *AGPAT2*, encoding 1-acyl-*sn*-glycerol-3-phosphate acyltransferase 2, were identified as causative genes for CGL. *Seipin* mutations were found in patients from families originating from Europe and the Middle East. *AGPAT2* mutations were found predominantly in African ancestry. However, no information is available on these genes in the pathogenesis of CGL in Asian ancestry. We examined the sequences of the entire coding region of *seipin* and *AGPAT2* in four Japanese CGL patients from independent families. Their average body fat content was 4.7 ± 0.5%, and the plasma leptin level was 1.15 ± 0.14 ng/ml. We identified a novel nonsense mutation of *seipin* at codon 275 (R275X). Of four CGL patients, three were homozygous for R275X. No *seipin* mutation was found in any exon in one patient. We did not find any *AGPAT2* mutations in our Japanese patients, suggesting that *AGPAT2* is a minor causative gene, if any, for CGL in Japanese. This is the first report on gene and phenotype analysis of CGL in Japanese. (*J Clin Endocrinol Metab* 89: 2360–2364, 2004)

CONGENITAL GENERALIZED LIPODYSTROPHY (CGL), Berardinelli-Seip syndrome, is characterized by a near total lack of adipose tissue from birth (1–3). Patients with CGL show severe insulin resistance, hypertriglyceridemia, and fatty liver. These metabolic abnormalities develop as a consequence of mass reduction of adipose tissue (4, 5). Leptin is an adipocyte-derived hormone that plays an important role in the regulation of glucose and lipid metabolism (6–8). Plasma leptin concentrations are markedly reduced in patients with lipodystrophy (9, 10). In this context, we and others (11, 12) demonstrated that transgenic overexpression of leptin or exogenous leptin administration reverses the metabolic abnormalities in different mouse models of lipoatrophic diabetes, indicating that the metabolic abnormalities in patients with lipodystrophy are caused mainly by a lack of leptin. However, the genetic defect that causes a failure of adipogenesis or adipocyte differentiation in CGL had long been unknown.

CGL has been suggested to be an autosomal recessive disorder. Recently, two causative genes for CGL were identified. One is a gene encoding a protein named seipin, whose function is unknown (13). The other is the *AGPAT2* gene encoding 1-acyl-*sn*-glycerol-3-phosphate acyltransferase 2 that belongs to the family of acyltransferases and catalyzes the biosynthesis of glycerophospholipids and triglyceride (14). The *seipin* gene is located in chromosome 11q13, and the *AGPAT2* gene is located in chromosome 9q34. Although there is no difference in the prevalence of metabolic disorders such as insulin resistance, hypertriglyceridemia, and fatty liver between patients with the *seipin* or *AGPAT2* mutation, CGL due to *seipin* mutation appears to be a more severe disease than that due to *AGPAT2* mutation, with a higher incidence of premature death and a lower prevalence of partial and/or delayed onset of lipodystrophy (15). Furthermore, patients with the *seipin* mutation have a higher prevalence of intellectual impairment than those with the *AGPAT2* mutation (15).

Seipin mutations were found in patients originating from Europe and the Middle East. *AGPAT2* mutations were found predominantly in African ancestry. However, no information is available about these genes in the pathogenesis of CGL in Asian subjects. The present study is the first report on gene and phenotype analysis of CGL in Japanese.

Subjects and Methods

Study subjects

Sequence analyses of *seipin* and *AGPAT2* were performed in four Japanese CGL patients (two men and two women). The clinical features and laboratory data of these patients are presented in Tables 1 and 2. All of these patients had a near total lack of body fat from birth. The study was approved by the ethical committee of Kyoto University Graduate School of Medicine. All subjects gave written informed consent for participating in the study.

Materials and methods

Genomic DNA was isolated from blood using InstaGene Whole Blood kit (Bio-Rad, Hercules, CA) according to the manufacturer's protocol.

Abbreviations: ANP, Atrial natriuretic peptide; BMI, body mass index; BNP, brain natriuretic peptide; CGL, congenital generalized lipodystrophy; IQ, intelligence quotient; MRI, magnetic resonance imaging; SNP, single nucleotide polymorphism.

JCEM is published monthly by The Endocrine Society (http://www.endo-society.org), the foremost professional society serving the endocrine community.

The coding regions of *seipin* and *AGPAT2* were amplified by PCR using gene-specific primers (13, 14) in seven and six fragments, respectively. PCR products were separated by electrophoresis in 2% agarose gel, purified, and sequenced directly by the dideoxy chain termination method with both forward and reverse primers on an ABI PRISM 310 Genetic Analyzer (PerkinElmer, PE Applied Biosystems, Foster City, CA). Genotyping of the patients with highly polymorphic microsatellite markers in chromosome 11q13 for the *seipin* locus and chromosome 9q34 for the *AGPAT2* locus was conducted with an ABI PRISM 310 Genetic Analyzer equipped with GeneScan analysis software (version 2.1, PerkinElmer).

The body mass index (BMI) was calculated as weight in kilograms divided by height in meters squared. Body fat was determined by dual energy x-ray absorptiometry. Body fat distribution was assessed using the whole body magnetic resonance imaging (MRI). MRI was performed using a 1.5-Tesla imaging device (Phillips Medical Systems, Best, The Netherlands). The entire body was surveyed using contiguous axial 10-mm slices and a relatively T1-weighted spin echo sequence. Blood samples were obtained after an overnight fast. Plasma leptin levels were determined by immunoassay using a commercial kit (Linco Research, Inc., St. Charles, MO). Blood glucose and triglyceride levels were determined according to standard methods with the use of automated equipment. Hemoglobin A_{1c} values were measured by ion exchange HPLC. Serum insulin levels were determined by immunoassays using reagents provided by Shibayagi Co. Ltd. (Gunma, Japan). The presence of hypertrophic cardiomyopathy was assessed using echocardiography, electrocardiography, and plasma atrial natriuretic peptide (ANP) and brain natriuretic peptide (BNP) levels. Plasma ANP and BNP levels were determined by immunoradiometric assay (Shionogi, Osaka, Japan) (16, 17). Fatty liver was diagnosed by both ultrasound and computed tomographic imaging. Intelligence quotient (IQ) was assessed using the Wechsler Adult Intelligence Scale-revised (18).

Statistical analysis

The average BMI in patient 1's family members with or without R275X heterozygous mutation were expressed as the mean ± SE. Comparison among groups was assessed by ANOVA and was completed by Fisher's probable least significant difference test.

Results

We studied four Japanese CGL patients from independent families. Clinical features of the patients are provided in Tables 1 and 2. These four patients showed generalized reduction or a near total lack of adipose tissue from birth. They presented with low body fat content and plasma leptin levels. Whole body MRI scans were available for patients 1, 3, and 4 (Fig. 1). All of these patients showed nearly total absence of sc fat throughout the body, including palm, sole, and head. They also showed near absence of ip fat. Retroorbital and bone marrow fat were preserved only in patient 4, not in patients 1 and 3. Patients 1, 3, and 4 had overt diabetes and markedly elevated hemoglobin A_{1c}values. Patient 1 was receiving insulin therapy. Patient 2 was not diabetic, although she presented with hyperinsulinemia. Patients 1 and 3 had both hypertriglyceridemia and fatty liver. In patient 2, hypertriglyceridemia and fatty liver had been observed in childhood. However, her fatty liver was improved on a strict low fat diet. Neither hypertriglyceridemia nor fatty liver was seen in patient 4. The prevalence of hypertrophic cardiomyopathy in CGL was reported as approximately 20% regardless of genotype (15). We assessed the presence of hypertrophic cardiomyopathy using echocardiography, electrocardiography, and plasma ANP and BNP levels. These results are presented in Table 3. Echocardiography indicated no apparent sign of hypertrophy in interventricular septal wall and left ventricular posterior wall. Electrocardiography indicated no sign of left ventricular hypertrophy. Plasma levels of ANP and, especially, BNP were elevated in patients with hypertrophic cardiomyopathy (19). Although the plasma BNP level in patient 3 was slightly elevated, all patients' levels of both ANP and BNP were almost within normal range. None of the four CGL patients had obvious hypertrophic cardiomyopathy. IQ was assessed in patients 1 and 4. Their IQs were 76 and 80, respectively, which were relatively low, but in the normal range. A formal assessment was not available for patients 2 and 3, but they also showed no distinct intellectual impairment that interfered with daily or school life. All four patients had mild to moderate acanthosis nigricans. Patient 2, who was 12 yr of age, had still not experienced menophania. Patient 3 experienced menophania at the age of 12 yr, but presented with oligomenorrhea and polycystic ovary in our study.

Sequence analysis of the entire coding regions of *seipin* and *AGPAT2* disclosed a novel homozygous C to T mutation at nucleotide 823 in exon 8 of *seipin* in patients 1, 2, and 3 (Fig. 2). This mutation predicts the substitution of arginine at codon 275 by the stop codon (R275X). Patient 4 had no mutation in the coding regions of the *seipin* gene. We did not find any AGPAT2 gene mutation in all four Japanese patients. The pedigrees of the patients are illustrated in Fig. 3. Consanguinity was recognized in the pedigrees of the patients with the *seipin* mutation, but not in the pedigree of patient 4. Although a DNA sample from the father of patient 3 was not available, the remaining five parents of the three patients with the *seipin* gene mutation were all heterozygous for the mutation. Parents showed no CGL phenotypes. Their BMI ranged from 23.5–26.3, and they were not diabetic. We also examined 10 family members of patient 1 for the R275X mutation and found six of them to be heterozygous (Fig. 2A). We found no significant difference in the average BMI be-

TABLE 1. Clinical features of patients with CGL

Patient no.	Sex	Age (yr)	BMI (kg/m^2)	Body fat (%)	Leptin (ng/ml)
1	M	19	20	5.0	1.23
2	F	13	16	3.3	1.05
3	F	23	21	5.7	1.50
4	M	29	14	4.7	0.82

TABLE 2. Metabolic characters of patients with CGL

Patient no.	DM	Age of onset of DM (yr)	Glucose (mg/dl)	Insulin (μU/ml)	HbA_{1c} (%)	Triglyceride (mg/dl)	Fatty liver
1	+	10	238	ND	8.8	547	+
2	−	−	82	49.0	6.0	180	−
3	+	5	268	17.2	11.8	318	+
4	+	12	142	5.2	10.3	69	−

+, Present; −, absent; DM, diabetes mellitus; HbA_{1c}, hemoglobin A_{1c}; ND, not determined.

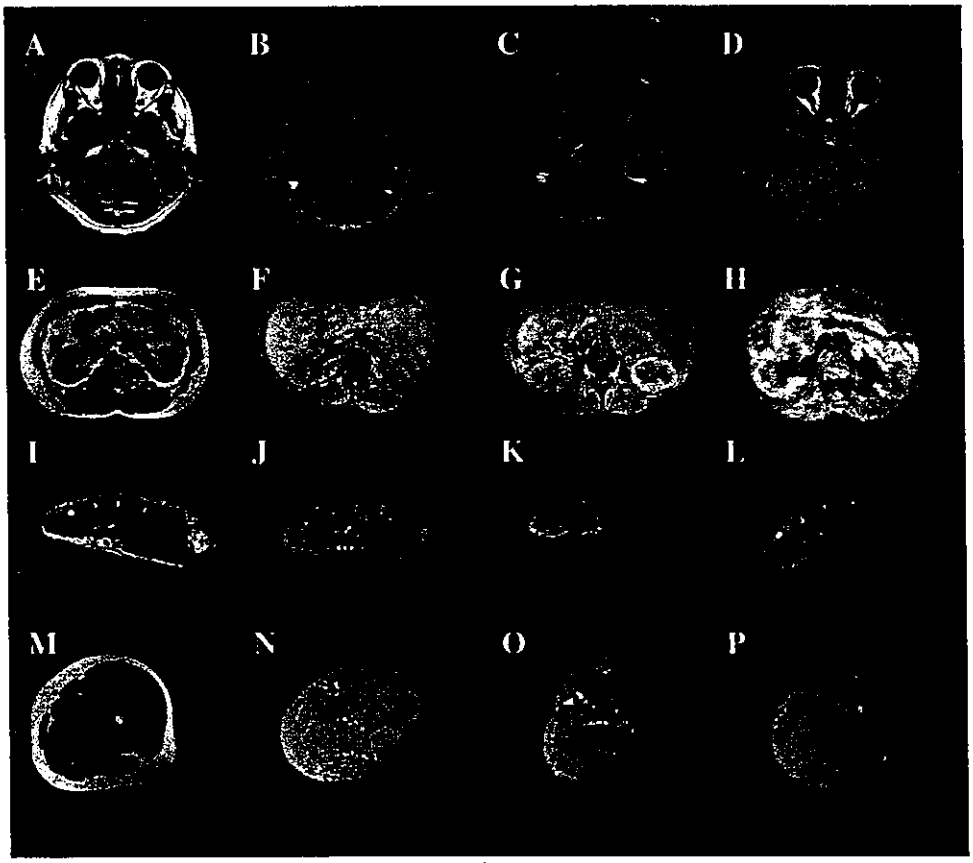

FIG. 1. T1-weighted magnetic resonance images at the levels of orbits (A–D), umbilicus (E–H), palm (I–L), and thigh (M–P) in the control (A, E, I, and M) and in patients 1 (B, F, J, and N), 3 (C, G, K, and O), and 4 (D, H, L, and P).

TABLE 3. Clinical parameters related to hypertrophic cardiomyopathy in patients with CGL

Patient no.	Echocardiography		ECG	ANP	BNP
	IVST (mm)	PWT (mm)	LVH	(pg/ml)	(pg/ml)
1	10	8	–	7.1	5>
2	9	8	–	9.4	9.2
3	9	9	–	14.5	16.3
4	7	7.5	–	15.0	5>

IVST, Interventricular septal wall thickness; PWT, left ventricular posterior wall thickness; ECG, electrocardiogram; LVH, left ventricular hypertrophy diagnosed based on the presence of tall left precardial R waves and deep right precardial S waves (SV1 + RV5 or RV6 >35 mm); –, absence.

tween the family members with or without the R275X heterozygous mutation (25.5 ± 3.6 and 27.8 ± 3.3 kg/m^2, respectively; $P = 0.33$). We also found no difference in the prevalence of diabetes mellitus between these two groups. Of 10 family members, one for each genotype had diabetes mellitus. These observations indicate that CGL caused by the *seipin* R275X mutation is inherited as an autosomal recessive fashion.

We investigated the genotype using microsatellite markers on *seipin* and *AGPAT2* loci and single nucleotide polymorphisms (SNPs) within the *seipin* gene (13, 20) (Table 4). Patients 1–3 were homozygous for the microsatellite markers flanking the *seipin* gene and the SNPs within the gene. In addition, they were disclosed to have the same genotype of microsatellite markers in this region and the SNPs. On the other hand, patient 4 was heterozygous for both *seipin* and *AGPAT2* loci.

Discussion

Seipin is homologous to cDNA of the mouse *Gng3lg* with unknown function, which is localized in the region of mouse chromosome 19 that is orthologous to human 11q (13, 21–23). Comparison between mouse and human sequences showed that the human cDNA contained an open reading frame of 1196 nucleotides, starting at position 345. Seipin is a predicted protein with 398 amino acids and more than two hydrophobic amino acid stretches, suggesting that it could be a *trans*-membrane protein. However, seipin has no similarity with other known proteins or consensus motif that could predict its function. Fourteen different *seipin* mutations, including R275X, have been identified to date (13, 15). Of these mutations, R275X is the most C-terminally located mutation. R275X results in a deletion of 124 amino acids of its C-terminal region. The patients with the homozygous R275X mutation show typical CGL phenotypes, suggesting that the C-terminal region of 124 amino acids could be important for the protein function, especially in adipogenesis or adipocyte differentiation. The metabolic phenotypes including insulin resistance and dyslipidemia in our subjects were similar to those observed in CGL subjects with the *seipin* mutation from other ethnic groups (13, 15). This suggests that the *seipin* gene mutation alone is sufficient for the onset of these metabolic abnormalities.

Of four patients we investigated, three had a homozygous mutation in the *seipin* gene, and their mutation was the same

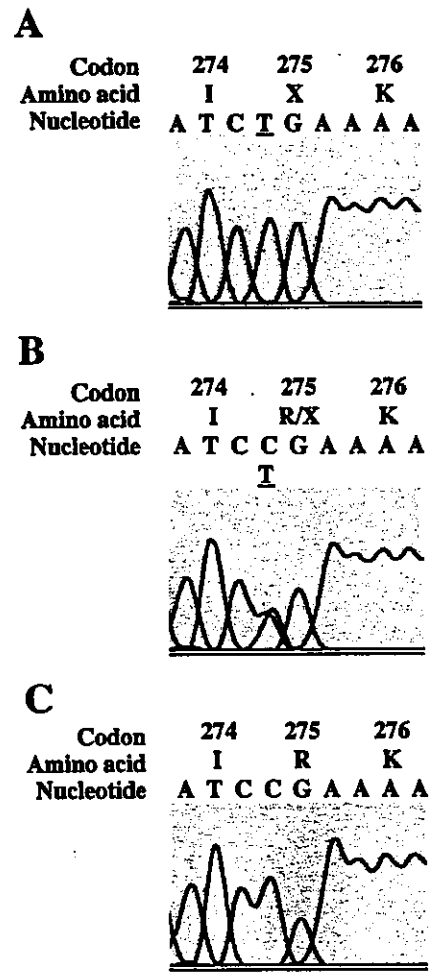

FIG. 2. Sequence analyses of the *seipin* gene. A, B, and C, Homozygous and heterozygous C to T mutations and normal sequence at nucleotide 823 in patient 1, his father, and his aunt.

R275X mutation in all of them. Although they were from independent families living in different remote regions in Japan, they had the same genotype of the microsatellite markers flanking the *seipin* gene and the SNPs within the gene. This demonstrates that they have a common ancestor in whom the R275X mutation was originated.

We did not find any mutations in the coding regions of *seipin* and *AGPAT2* in patient 4. Genotype analysis using microsatellite markers and SNPs revealed that he is heterozygous for *seipin* and *AGPAT2* loci. His phenotype, without hypertriglyceridemia and fatty liver, is atypical for CGL with *seipin* or *AGPAT2* mutation. Further, retroorbital and bone marrow fats are preserved only in patient 4 in the present study. Taken together, it is unlikely that *seipin* and *AGPAT2* genes link to his disease, although we cannot completely exclude the possibility that he has compound heterozygous mutation in noncoding regions of the genes. In addition, the generalized deficiency of body fat and the typically lipoatrophic face were noticed at birth, and autoimmune or causative disease has not been demonstrated in patient 4. These findings indicate the possible existence of another locus for CGL.

We did not find any *AGPAT2* mutations in these four

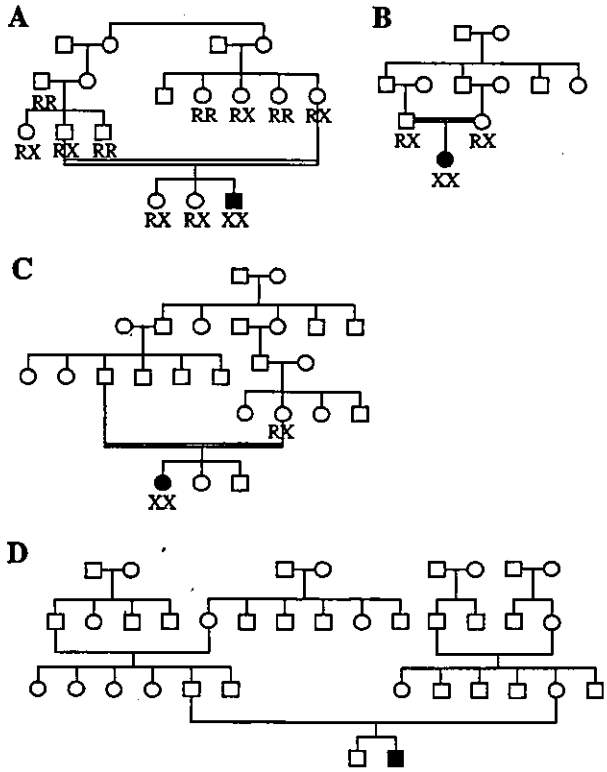

FIG. 3. Pedigrees of patients 1 (A), 2 (B), 3 (C), and 4 (D). *Squares* and *circles* indicate males and females, respectively. The probands are shown as *filled symbols*, and other family members are shown as *unfilled symbols*. The R275X homozygous mutation is shown as XX, the heterozygous mutation is shown as RX, and the wild type is shown as RR.

TABLE 4. Status of microsatellites and SNPs at the *seipin* and *AGPAT2* loci in patients

Microsatellites	Patient no.			
	1	2	3	4
Seipin				
D11S986	1,2	4,4	2,2	1,4
D11S4191	2,5	6,6	5,5	2,7
D11S1765	1,1	1,1	1,1	1,1
D11S4076	2,2	3,3	2,2	2,3
CA10	6,6	6,6	6,6	1,5
CA9	1,1	1,1	1,1	1,2
D11S480	1,1	1,1	1,1	1,1
D11S1883	2,2	2,2	1,1	1,2
D11S4205	1,1	3,3	3,3	3,3
PYGM		2,2	3,4	4,5
SNPs				
Int5/+69	G,G	G,G	G,G	A,G
Int5/−49	C,C	C,C	C,C	T,C
Ex9/65	A,A	A,A	A,A	A,G
AGPAT2				
D9S164	4,5	1,4	3,4	3,5
D9S1818	2,3	2,3	1,1	2,3
D9S1826	2,7	1,4	4,5	2,7
D9S1838	2,2	2,6	1,3	2,4
D9S158	1,1	1,1	3,3	2,5

patients. Although the number of subjects we examined was small, these observations indicate that *AGPAT2* is a minor causative gene for CGL in the Japanese people. We also elucidated that one of four patients is without *seipin* or

AGPAT2 mutations. He did not present a lipid metabolic disturbance until now, although dyslipidemia is one of the major phenotypes of CGL caused by *seipin* or *AGPAT2* mutations. This observation is consistent with the presence of another CGL-associated gene (20). This is the first report of gene and phenotype analysis of CGL in the Japanese population.

Acknowledgments

Drs. Koji Kitamura, Katsuhiko Tachibana, Masanori Adachi, and Yoichiro Oda originally referred the patients for assessment. We thank Jocelyne Magre, Ph.D., for helpful comments about gene analysis.

Received July 11, 2003. Accepted February 12, 2004.

Address all correspondence and requests for reprints to: Dr. Ken Ebihara, Department of Medicine and Clinical Science, Kyoto University Graduate School of Medicine, 54 Shogoin Kawahara-cho, Sakyo-ku, Kyoto 606-8507, Japan. E-mail: kebihara@kuhp.kyoto-u.ac.jp.

This work was supported by grants from the Japanese Ministry of Health, Welfare, and Labor; Kato Memorial Bioscience Foundation; a grant-in-aid from the Japan Medical Association; the Japan Research Foundation for Clinical Pharmacology; and a study grant from the Japan Insulin Study Group.

K.E. and T.K. contributed equally to this work.

Present address for Y.O.: Department of Molecular Medicine and Metabolism, Medical Research Institute, Tokyo Medical and Dental University, Tokyo 101-0062, Japan.

References

1. **Berardinelli W** 1954 An undiagnosed endocrinometabolic syndrome: report of two cases. J Clin Endocrinol Metab 14:193–204
2. **Seip M** 1959 Lipoatrophy and gigantism with associated endocrine manifestations: a new diencephalic syndrome? Acta Paediatr Scand 48:555–574
3. **Seip M, Trygstad O** 1996 Generalised lipodystrophy, congenital and acquired (lipoatrophy). Acta Paediatr 413(Suppl):2–28
4. **Moitra J, Mason MM, Olive M, Krylov D, Gavrilova O, Marcus-Samuels B, Feigelbaum L, Lee E, Aoyama T, Eckhaus M, Reitman ML, Vinson C** 1998 Life without white fat: a transgenic mouse. Genes Dev 12:3168–3181
5. **Shimomura I, Hammer RE, Richardson JA, Ikemoto S, Bashmakov Y, Goldstein JL, Brown MS** 1998 Insulin resistance and diabetes mellitus in transgenic mice overexpressing nuclear SREBP-1c in adipose tissue: model for congenital generalized lipodystrophy. Genes Dev 12:3182–3194
6. **Kamohara S, Burcellin R, Hallas JL, Friedman JM, Charron MJ** 1997 Acute stimulation of glucose metabolism in mice by leptin treatment. Nature 389: 374–377
7. **Ogawa Y, Masuzaki H, Hosoda K, Aizawa-Abe M, Suga J, Suda M, Ebihara K, Iwai H, Matsuoka N, Satoh N, Odaka H, Kasuga H, Fujisawa Y, Inoue G, Nishimura H, Yoshimasa Y, Nakao K** 1999 Increased glucose metabolism and insulin sensitivity in transgenic skinny mice overexpressing leptin. Diabetes 48:1822–1829
8. **Shimabukuro M, Koyama K, Chen G, Wang M-Y, Trieu F, Lee Y, Newgard CB, Unger RH** 1997 Direct antidiabetic effect of leptin through triglyceride depletion of tissues. Proc Natl Acad Sci USA 94:4637–4641
9. **Andreeli F, Hanaire-Broutin H, Laville M, Tauber JP, Riou JP, Thivolet C** 2000 Normal reproductive function in leptin-deficient patients with lipoatrophic diabetes. J Clin Endocrinol Metab 85:715–719
10. **Pardini VC, Victoria IM, Rocha SM, Andrade DG, Rocha AM, Pieroni FB, Milagres G, Purish S, Velho G** 1998 Leptin levels, b-cell function, and insulin sensitivity in families with congenital and acquired generalized lipoatrophic diabetes. J Clin Endocrinol Metab 83:503–508
11. **Ebihara K, Ogawa Y, Masuzaki H, Shintani M, Miyanaga F, Aizawa-Abe M, Hayashi T, Hosoda K, Inoue G, Yoshimasa Y, Gavrilova O, Reitman ML, Nakao K** 2001 Transgenic overexpression of leptin rescues insulin resistance and diabetes in a mouse model of lipoatrophic diabetes. Diabetes 50:1440–1448
12. **Shimomura I, Hammer RE, Ikemoto S, Brown MS, Goldstein JL** 1999 Leptin reverses insulin resistance and diabetes mellitus in mice with congenital lipodystrophy. Nature 401:73–76
13. **Magre J, Delepine M, Khallouf E, Gedde-Dahl Jr T, Van Maldergem L, Sobel E, Papp J, Meier M, Megarbane A, BSCL Working Group, Lathrop M, Capeau J** 2001 Identification of the gene altered in Berardinelli-Seip congenital lipodystrophy on chromosome 11q13. Nat Genet 28:365–370
14. **Agarwal AK, Arioglu E, de Almeida S, Akkoc N, Taylor SI, Bowcock AM, Barnes RI, Garg A** 2002 AGPAT2 is mutated in congenital generalized lipodystrophy linked to chromosome 9q34. Nat Genet 31:21–23
15. **Van Maldergem L, Magre J, Khallouf TE, Gedde-Dahl Jr T, Delepine M, Trygstad O, Seemanova E, Stephenson T, Albott CS, Bonnici F, Panz VR, Medina J-L, Bogalho P, Huet F, Savasta S, Verloes A, Robert J-J, Loret H, de Kerdanet M, Tubiana-Rufi N, Megarbane A, Maassen J, Polak M, Lacombe D, Kahn CR, Silveria EL, D'Abronzo FH, Grigorescu F, Lathrop M, Capeau J, O'Rahilly S** 2002 Genotype-phenotype relationships in Berardinelli-Seip congenital lipodystrophy. J Med Genet 39:722–733
16. **Mukoyama M, Nakao K, Sugawa H, Morii N, Sugawara A, Yamada T, Itoh H, Shiono S, Saito Y, Arai H** 1988 A monoclonal antibody to α-human atrial natriuretic polypeptide. Hypertension 12:117–121
17. **Itoh H, Nakao K, Saito Y, Yamada T, Shirakami G, Mukoyama M, Arai H, Hosoda K, Suga S, Minamino N, Kangawa K, Matsuo H, Imura H** 1989 Radioimmunoassay for brain natriuretic peptide (BNP) detection of BNP in canine brain. Biochem Biophys Res Commun 158:120–128
18. **Ryan JJ, Prifitera A, Larsen J** 1982 Reliability of the WAIS-R with a mixed patient sample. Percept Mot Skills 55:1277–1278
19. **Yoshibayashi M, Kamiya T, Saito Y, Matsuo H** 1993 Increased plasma levels of brain natriuretic peptide in hypertrophic cardiomyopathy. N Engl J Med 329:433–434
20. **Heathcote K, Rajab A, Magre J, Syrris P, Besti M, Patton M, Delepine M, Lathrop M, Capeau J, Jeffery S** 2002 Molecular analysis of Berardinelli-Seip congenital lipodystrophy in Oman; evidence for multiple loci. Diabetes 51: 1291–1293
21. **Downes GB, Copeland NG, Jenkins NA, Gautam N** 1998 Structure and mapping of the G protein γ3 subunit gene and a divergently transcribed novel gene, gng3lg. Genomics 53:220–230
22. **Yu W, Andersson B, Worley KC, Muzny DM, Ding Y, Liu W, Ricafrente JY, Wentland MA, Lennon G, Gibbs RA** 1997 Large-scale concatenation cDNA sequencing. Genome Res 7:353–358
23. **Inoue S, Sano H, Ohta M** 2000 Growth suppression of *Escherichia coli* by induction of expression of mammalian genes with transmembrane or ATPase domain. Biochem Biophys Res Commun 268:553–561

JCEM is published monthly by The Endocrine Society (http://www.endo-society.org), the foremost professional society serving the endocrine community.

0018-7227/04/$15.00/0
Printed in U.S.A.

Endocrinology 145(2):951–958

doi: 10.1210/en.2003-0816

Androgen Contributes to Gender-Related Cardiac Hypertrophy and Fibrosis in Mice Lacking the Gene Encoding Guanylyl Cyclase-A

YUHAO LI, ICHIRO KISHIMOTO, YOSHIHIKO SAITO, MASAKI HARADA, KOICHIRO KUWAHARA, TAKEHIKO IZUMI, ICHIRO HAMANAKA, NOBUKI TAKAHASHI, RIKA KAWAKAMI, KEIJI TANIMOTO, YASUAKI NAKAGAWA, MICHIO NAKANISHI, YUICHIRO ADACHI, DAVID L. GARBERS, AKIYOSHI FUKAMIZU, AND KAZUWA NAKAO

Department of Medicine and Clinical Science (Y.L., I.K., Y.S., M.H., K.K., T.I., I.H., N.T., R.K., K.T., Y.N., M.N., Y.A., K.N.), Kyoto University Graduate School of Medicine, Kyoto 606-8501, Japan; Howard Hughes Medical Institute and Department of Pharmacology (D.L.G.), University of Texas, Southwestern Medical Center at Dallas, Dallas, Texas 75390; and Center for Tsukuba Advanced Research Alliance (A.F.), Institute of Applied Biochemistry, University of Tsukuba, Tsukuba, Ibaraki 305-8571, Japan

Myocardial hypertrophy and extended cardiac fibrosis are independent risk factors for congestive heart failure and sudden cardiac death. Before age 50, men are at greater risk for cardiovascular disease than age-matched women. In the current studies, we found that cardiac hypertrophy and fibrosis were significantly more pronounced in males compared with females of guanylyl cyclase-A knockout (GC-A KO) mice at 16 wk of age. These gender-related differences were not seen in wild-type mice. In the further studies, either castration (at 10 wk of age) or flutamide, an androgen receptor antagonist, markedly attenuated cardiac hypertrophy and fibrosis in male GC-A KO mice without blood pressure change. In contrast, ovariectomy (at 10 wk of age) had little effect. Also, chronic testosterone infusion increased cardiac mass and fibrosis in ovariectomized GC-A mice. None of the treatments affected cardiac mass or the extent of fibrosis in wild-type mice. Overexpression of mRNAs encoding atrial natriuretic peptide, brain natriuretic peptide, collagens I and III, TGF-β1, TGF-β3, angiotensinogen, and angiotensin converting enzyme in the ventricles of male GC-A KO mice was substantially decreased by castration. The gender differences were virtually abolished by targeted deletion of the angiotensin II type 1A receptor gene (AT1A). Neither castration nor testosterone administration induced any change in the cardiac phenotypes of double-KO mice for GC-A and AT1A. Thus, we suggest that androgens contribute to gender-related differences in cardiac hypertrophy and fibrosis by a mechanism involving AT1A receptors and GC-A. (*Endocrinology* 145: 951–958, 2004)

MYOCARDIAL HYPERTROPHY IS prevalent in a substantial portion of individuals with essential hypertension (1, 2), and it is recognized as an independent risk factor for congestive heart failure and sudden cardiac death (3). Extended cardiac fibrosis results in increased myocardial stiffness, causing ventricular dysfunction and, ultimately, heart failure (4). Significant gender-related differences in the cardiovascular system are now well documented, and before the age of 50, men are at greater risk for cardiovascular diseases than age-matched women (5–9). However, the precise mechanism underlying gender-related differences in cardiac diseases is not fully understood. The results of both *in vitro* and *in vivo* studies indicate that sex steroids play a key role in the development of cardiac structural abnormalities. Estrogen and androgen receptors are present in myocardial tissues (10–12). Estradiol has antiproliferative effects on cardiac fibroblasts (13) and vascular smooth-muscle cells (14, 15), whereas androgens increase proliferation of vascular smooth-muscle cells (16). Studies using sinoaortic denervation-induced cardiac hypertrophy in rats have also shown that testosterone facilitates hypertrophy but estradiol inhibits it (17). A less severe model of cardiac hypertrophy in rats (swimming- or hypertension-induced) failed to confirm the antiproliferative effect of estradiol (18). Moreover, not all males, whether human or experimental animal, develop gender-related cardiac abnormalities. Somjen and colleagues (15) reported a biphasic proliferative response for both estrogen and testosterone in vascular smooth muscle and endothelial cells. It, therefore, is unclear how gender-induced changes in cardiac structural pathology are made manifest.

Mice lacking guanylyl cyclase A (GC-A), a natriuretic peptide receptor, exhibit salt-resistant hypertension, myocardial hypertrophy and interstitial fibrosis, and sudden death (before the age of 6 months) (19–20). In the present study, we found that male GC-A knockout (KO) mice show more pronounced cardiac hypertrophy and fibrosis compared with female GC-A KO mice and that gender-related differences are not seen in wild-type (WT) mice. Additionally, we found that these gender-related differences are attenuated either by castration or flutamide, an androgen receptor (AR) antagonist, and abolished by genetic disruption of angiotensin

Abbreviations: ACE, Angiotensin converting enzyme; Agt, angiotensinogen; Ang, angiotensin; ANP, atrial natriuretic peptide; AR, androgen receptor; AT1A, Ang II type 1A; BNP, brain natriuretic peptide; BW, body weight; GC-A, guanylyl cyclase-A; HR, heart rate; KO, knockout; LVW, left ventricular weight; OVX, ovariectomy; SBP, systolic blood pressure; WT, wild-type.

Endocrinology is published monthly by The Endocrine Society (http://www.endo-society.org), the foremost professional society serving the endocrine community.

(Ang) II type 1A (AT1A) receptors in male GC-A KO mice. We propose that androgens contribute to gender-related differences in cardiac structure and that the AT1A receptor and GC-A are involved in a reciprocal fashion.

Materials and Methods

Animals and treatments

All experimental procedures were carried out in accordance with Kyoto University standards for animal care. GC-A KO mice were originally generated at the University of Texas, Southwestern Medical Center at Dallas and Howard Hughes Medical Institute. Mice were housed in groups of three to five per cage under climate-controlled conditions with a 12-h light/dark cycle and were provided with standard food (CRF-1; Oriental Yeast Co., Ltd, Tokyo, Japan) and water *ad libitum*. The WT (GC-A+/+, AT1A+/+), AT1A KO (GC-A+/+, AT1A−/−), GC-A KO (GC-A−/−, AT1A+/+), and double-KO (GC-A−/−, AT1A−/−) mice used in these experiments were generated from heterozygous (GC-A+/−, AT1A +/−) mice after crossing of single GC-A KO (19) and AT1A KO (21) mice. The genetic background of the original GC-A KO and AT1A KO mice was C57BL/6. Genotypes were determined before and verified after experimentation using PCR. Comparisons of age and body weight (BW) between the KO and WT mice were made among littermates. Also comparisons of age, body weight, and systolic blood pressure (SBP) between control and treated mice were performed.

Measurement of heart rate (HR) and SBP

HR and SBP were measured in conscious mice using a computerized tail-cuff method (Softron Co., Ltd., Tokyo, Japan) (19, 21). Briefly, mice were restrained in a pocket and warmed at 38 C. HR and SBP were measured at 1000–1400 h and calculated as the average of six sessions per day after mice were adapted to the apparatus for 5 d. The validity of this system has been established previously in our laboratory (22).

Measurement of left ventricular weight (LVW) and interstitial fibrosis

After animals were killed by cervical dislocation under anesthesia with ether at 16 wk of age, the hearts were dissected out, LVW was measured, and its ratio to BW (LVW/BW) was calculated and used as an index of ventricular hypertrophy. The left ventricles were then fixed in 10% formalin and prepared for routine histological examination. To determine the degree of collagen fiber accumulation, we randomly selected 20 fields in three individual sections and calculated the ratio of the areas of van Gieson-stained interstitial fibrosis to the total left ventricular area using image analysis software and a Zeiss KS400 system; perivascular fibrosis was excluded in the present study.

mRNA analysis

Total mRNA was prepared from the left ventricle using TRIzol (Life Technologies Inc., Rockville, MD). Expression of mRNAs encoding atrial natriuretic peptide (ANP), brain natriuretic peptide (BNP), collagens I and III, TGF-β1, TGF-β3, angiotensinogen (Agt), and Ang converting enzyme (ACE) was evaluated using quantitative RT-PCR in a 7700 sequence detector (ABI PRISM, Applied Biosystems, Foster City, CA). The oligonucleotide primers are shown in Table 1. Glyceraldehyde-3-phosphate dehydrogenase mRNA was also amplified with specific primers and probe (Applied Biosystems).

Experimental protocols

We first compared the gender-related differences in the phenotypes of 16-wk-old GC-A KO and WT mice (n = 7–9 per group). HR and SBP were measured, and LVW, LVW/BW, and left ventricular fibrosis were calculated, after which related mRNA expression was analyzed.

To evaluate the involvement of estrogen in gender-related differences, we compared the phenotypes of sham-operated and ovariectomized (OVX) mice (n = 7–9 per group). Under anesthesia with ether, the ovaries of 10-wk-old female mice were exteriorized, ligated, and removed *via* bilateral paralumbar incisions, which were then closed with sutures. In sham mice, the ovaries were exteriorized and replaced, and the incisions were closed. Six weeks later, HR and SBP were measured, and the animals were killed.

To investigate the effects of androgens, male mice at 10 wk of age (n = 7–9 per group) were castrated using the trans-scrotal approach. Sham castration consisted of exteriorizing and replacing the testes. As in females, 6 wk later, HR and SBP were measured, and the animals were killed.

To confirm the role of androgen, we ovariectomized female WT and GC-A KO mice (n = 6–7 per group) under anesthesia with ether at 10 wk of age and sc implanted a testosterone pellet (25.0 mg/pellet, 60-darelease, catalog item SA-151) or vehicle pellet (placebo for testosterone, catalog item SC-111) (Innovative Research of America, Sarasota, FL) between the shoulders. Six weeks later, the animals were killed after HR and SBP were measured.

We further confirmed the role of androgens by chronically blocking AR with flutamide (23–24). Flutamide (Sigma Chemical Co., St. Louis, MO; 8 mg/kg·d, dissolved in polyethylene glycol 300) was sc infused for 6 wk using an osmotic mini-pump (model 2002, Alza Corp., Mountain View, CA) at 10 wk of age in male animals (n = 7–9 per group). The mini-pumps were sc implanted under the mice were anesthetized with

TABLE 1. Primer and probe sequences for RT-PCR assays

mRNA	Probe	Primers[a]
ANP	TGTACAGTGCGGTGTCCAACACAGAT	*f*GCCATATTGGAGCAAATCCT
		*r*GCAGGTTCTTGAAATCCATCA
BNP	TGCAGAAGCTGCTGGAGCTGATAAGA	*f*CCAGTCTCCAGAGCAATTCAA
		*r*GCCATTTCCTCCGACTTTT
AT1A	CCGGAATTCAACGCTCCCCA	*f*GTTTGCGCTTTTCATTACGAGT
		*r*TCTTGGTTAGGCCCAGTCCT
ACE	CACATCCCAAACGTGACACCGTACAT	*f*CGGAATGAAACCCATTTTGA
		*r*GCACAAAGCTCACGAAGTACC
Agt	AGGTTCTCAATAGCATCCTCCTCGAACTC	*f*CATTGGTGACACCAACCCC
		*r*GCTGTTCCTCCTCTCCTGCT
TGF-β1	AGCGCATCGAAGCCATCCG	*f*GACGTCACTGGAGTTGTACGG
		*r*GCTGAATCGAAAGCCCTGT
TGF-β3	CGGATGAGCACATAGCCAAGCA	*f*TTGAGCTCTTCCAGATACTTCG
		*r*TTCTTGCCACCTATGTAGCG
Collagen I	CACGGCTGTGTGCGATGACG	*f*GTCCCAACCCCCAAAGAC
		*r*CATCTTCTGAGTTTGGTGATACGT
Collagen III	TCCCACTCTTATTTTGGCACAGCAGTC	*f*TGGTTTCTTCTCACCCTTCTTC
		*r*TGCATCCCAATTCATCTACGT

Sequences are listed 5′ to 3′.

[a] Forward primers are designated by *f* and reverse primers by *r*.

ether and changed with new ones every 2 wk. Control mice were administered only vehicle. Six weeks later, the animals were analyzed.

To assess the involvement of the AT1A receptors in GC-A disruption-induced gender difference, we deleted AT1A receptor by the described method above. At 16 wk of age, the animals (n = 5–9 per group) were analyzed.

To further support the conclusion of AT1A receptor involvement, we castrated male double-KO mice (10 wk old; n = 5–6 per group) and chronically infused exogenous testosterone and analyzed the animals by the described methods above.

Statistical analysis

All results are expressed as means ± SEM. Data were analyzed by one-facter ANOVA. If a statistically significant effect was found, the Newman-Keuls test was performed to isolate the difference between the groups. Values of $P < 0.05$ were considered statistically significant.

Results

GC-A deficiency induces gender-related cardiac differences

Targeted deletion of GC-A led to increased LVW/BW ratios in both male and female mice. However, the effect was greater in males (58% increase *vs.* 33% increase in females; Fig. 1A). In contrast, in WT mice, there was no difference in LVW/BW ratio in males *vs.* females (Fig. 1A). In addition, male GC-A KO mice, but not WT mice, exhibited higher levels of left ventricular fibrosis than did females (378% *vs.* 44%, respectively; Fig. 1, B and C). On the other hand, there was no gender-related difference in HR (WT female 599.6 ± 26.1 *vs.* male 619.0 ± 52.4 beats/min; GC-A KO female 574.5 ± 25.9 *vs.* male 571.3 ± 28.1 beats/min; n = 7–9 per group) or in SBP (WT female 118.4 ± 1.7 *vs.* male 113.2 ± 3.4 mm Hg; GC-A KO female 140.0 ± 3.4 *vs.* male 147.4 ± 2.2 mm Hg; n = 7–9 per group) in either genotype. Male mice weighed more than females, but there was no difference between genotypes [WT female 25.0 ± 0.9 *vs.* male 32.3 ± 1.6 g ($P < 0.05$); GC-A KO female 25.1 ± 0.8 *vs.* male 31.6 ± 1.9 g ($P < 0.05$); n = 7–9 per group].

OVX has little effect in the heart

To elucidate a possible mechanism by which GC-A could prevent gender-related difference in the heart, we first investigated the effects of estrogen depletion. OVX had no effect on HR (WT sham 599.6 ± 26.1 *vs.* OVX 590.4 ± 17.9 beats/min; GC-A KO sham 574.5 ± 25.9 *vs.* OVX 582.3 ± 14.1 beats/min; n = 7–9 per group), SBP (WT sham 118.4 ± 1.7 *vs.* OVX 112.0 ± 2.2 mm Hg; GC-A KO sham 140.6 ± 3.4 *vs.* OVX 137.7 ± 3.0 mm Hg; n = 7–9 per group), LVW/BW ratio, ventricular fibrosis in either mouse type (Fig. 1, A–C), or BW (WT sham 25.0 ± 0.9 *vs.* OVX 25.6 ± 0.8 g; GC-A KO sham 25.1 ± 0.8 *vs.* OVX 25.1 ± 1.6 g; n = 7–9 per group).

Neither castration nor administration of an AR antagonist diminishes cardiac hypertrophy and fibrosis in male GC-A KO mice, whereas testosterone infusion increases cardiac hypertrophy and fibrosis in OVX GC-A mice

In contrast to OVX, removal of testes was associated with a marked reduction in the LVW/BW ratio and in ventricular fibrosis in GC-A KO mice (by 20.5 and 44.7%, respectively) but not to levels comparable to those seen in WT mice. Castration had no effect in WT mice (Fig. 1). Castration reduced BW in male WT as well as in male GC-A KO mice [WT 5.7 ± 0.5 *vs.* 2.1 ± 0.4 g ($P < 0.05$), and GC-A KO 6.6 ± 0.9 *vs.* 2.7 ± 0.6 g ($P < 0.05$) for sham and castrated groups, respectively; n = 7–9 per group]. Castration had no effect on HR (WT 619.0 ± 52.4 *vs.* 606.2 ± 45.9 beats/min, and GC-A KO 571.3 ± 28.1 *vs.* 600.2 ± 13.2 beats/min, for sham and castrated groups, respectively; n = 7–9 per group) or SBP

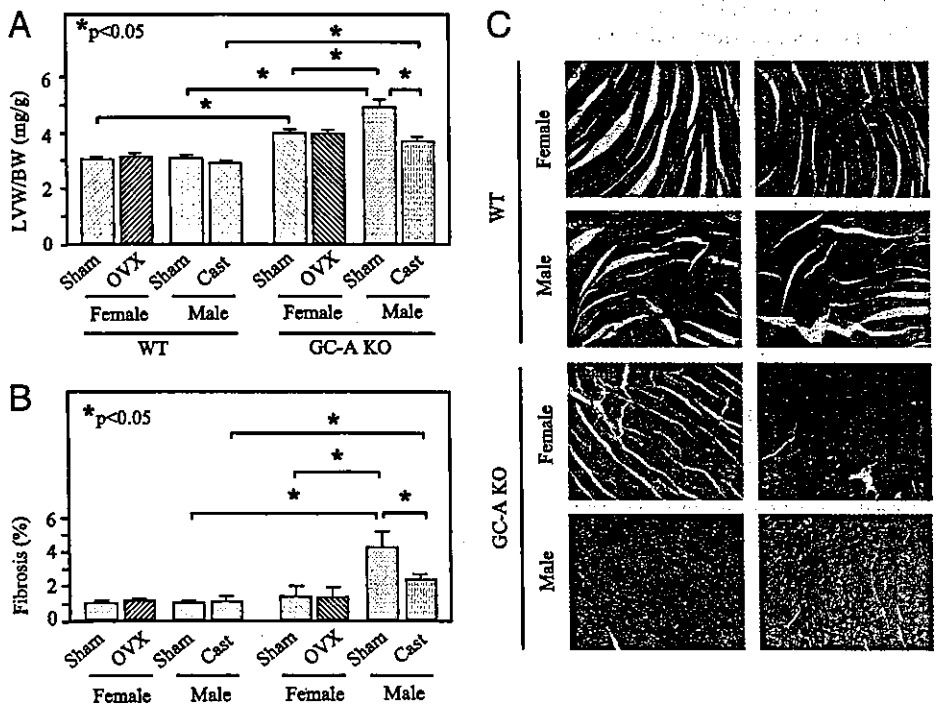

FIG. 1. GC-A disruption-induced gender-related differences in cardiac hypertrophy and fibrosis were inhibited by castration in male (Cast), but not in female (OVX) mice that were castrated at 10 wk and analyzed at 16 wk of age. The ratio of the areas of van Gieson-stained interstitial fibrosis to the total left ventricular area was calculated using image analysis software and a Zeiss KS400 system. A, LVW/BW ratio; B, relative levels of left ventricular fibrosis; C, photomicrographs showing representative examples of cardiac fibrosis (red) (magnification, ×200). Values are means ± SEM; n = 7–9 per group; *, $P < 0.05$.

(WT 113.2 ± 3.4 *vs.* 105.8 ± 4.2 mm Hg, and GC-A KO 147.4 ± 2.2 *vs.* 142.2 ± 6.3 mm Hg, for sham and castrated groups, respectively; n = 7–9 per group). The AR antagonist flutamide had similar effects to castration on LVW/BW, fibrosis (Fig. 2), HR (data not shown), and SBP (data not shown). In contrast, chronic infusion of testosterone increased LVW/BW ratio (by 20%) and cardiac fibrosis (by 114%) in OVX GC-A mice but not in OVX WT mice (Fig. 3). Testosterone treatment was also associated with increased BW in GC-A KO but not in WT mice]WT 2.6 ± 0.3 *vs.* 3.2 ± 0.3 g ($P < 0.05$), and GC-A KO 2.9 ± 0.2 *vs.* 5.2 ± 0.5 g ($P < 0.05$), for sham and testosterone-treated groups, respectively; n = 6–9 in each group[. HR and SBP were not affected by testosterone treatment (data not shown).

Gender-related difference in molecular expression profile

Basal left ventricular levels of ANP, BNP, collagen I, collagen III, TGF-β1, and TGF-β3 mRNAs were all higher in male than female GC-A KO mice. Castration of males decreased mRNA expression of these molecules to levels seen in females (Fig. 4). Again, no gender-related difference or castration-associated effects were seen in WT mice (Fig. 4). In contrast to the above mentioned genes, the levels of Agt and ACE mRNAs were higher in males than in females, and castration of males strongly suppressed their expression, and their levels were comparable in both genotypes of mice.

Deletion of AT1A abolishes gender-related cardiac differences

Deletion of the AT1A gene in GC-A KO mice reduced LVW/BW in both male and female mice, but the effects were more pronounced in the males (by 34 and 32.7% in males *vs.* 18 and 23.5% in females, respectively). AT1A deletion also markedly reduced cardiac fibrosis in male GC-A KO mice (by 57.5%). Gender-related cardiac differences (LVW/BW and fibrosis) were evident only in GC-A KO mice, but not in WT (as above), AT1A KO or double-KO mice (Fig. 5).

Castration or testosterone infusion fails to induce changes in cardiac mass and fibrosis in male double-KO mice

In contrast to the data obtained in GC-A KO mice (see above), neither castration nor testosterone infusion affected cardiac mass or the level of fibrosis in male double-KO mice (data not shown). Similarly, HR and SBP were unaffected by either castration or testosterone replacement (data not shown).

Discussion

As previous literatures documented significant gender-related differences in cardiovascular function and geometry (6, 7), the present study demonstrates that male GC-A KO mice show more marked left ventricular hypertrophy and severe interstitial fibrosis than female ones. Considering the protective effects of estrogen on the cardiovascular system (25, 26), we first investigated the effects of estrogens on the gender-related difference in the GC-A KO mouse hearts. Although OVX had little effect on cardiac mass and fibrosis in both WT and GC-A KO mice, there are still some possibilities that have not been addressed, such as, first, the fact that the effects of estrogen deprivation in women are not immediate; they develop over years, meaning that the 6-wk period of estrogen deprivation may be insufficient. Second, phytoestrogens are found in over 300 plants, including some used in human and animal diets (27–29). They can bind to the estrogen receptor and induce estrogen-like effects in animals, humans, and cells in culture. In the present study, we cannot exclude the possibility that the chow of mice may contain phytoestrogens, which may protect from (or limit) the effects of OVX. Therefore, the role of estrogen in gender-related cardiac difference observed in GC-A KO mice should be further clarified.

Next, we examined the effects of androgens. ARs are widely distributed in the cardiovascular system, where they have been identified on aortic, peripheral vascular, ventricular, and atrial myocytes (30), and were recently shown to mediate robust, testosterone-induced hypertrophic responses in cardiac myocytes (12). Nevertheless, although virtually all men have much higher levels of androgens than women do, not all men exhibit more severe cardiac hypertrophy and fibrosis. In the present study, significant gender-related differences in cardiac abnormalities were observed only in GC-A KO mice. In addition, it is notable that both castration and AR antagonist markedly diminished cardiac hypertrophy and fibrosis in male GC-A KO mice, and chronic

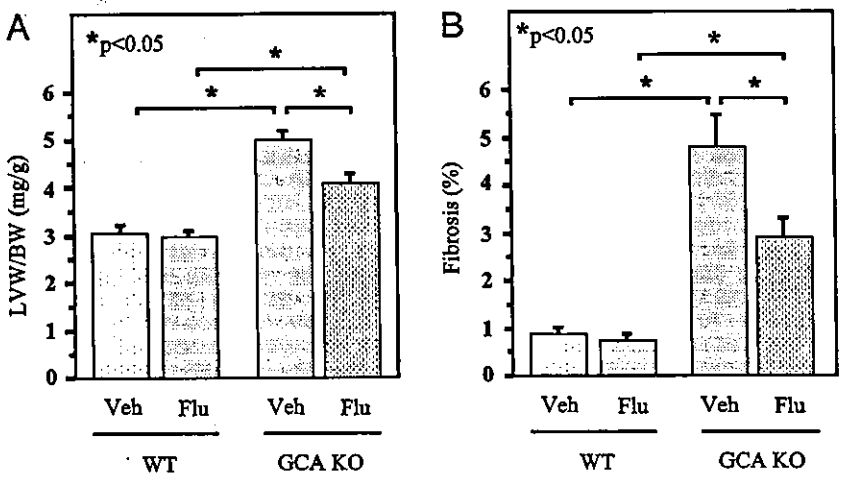

FIG. 2. Chronic AR blockade with flutamide was associated with decreased LVW/BW (A) and left ventricular fibrosis (B) in male GC-A KO mice. Flutamide (Flu; 8 mg/kg·d) or vehicle (Veh) was sc infused for 6 wk starting at 10 wk of age. Values are mean ± SEM; n = 7–9 per group; *, $P < 0.05$.

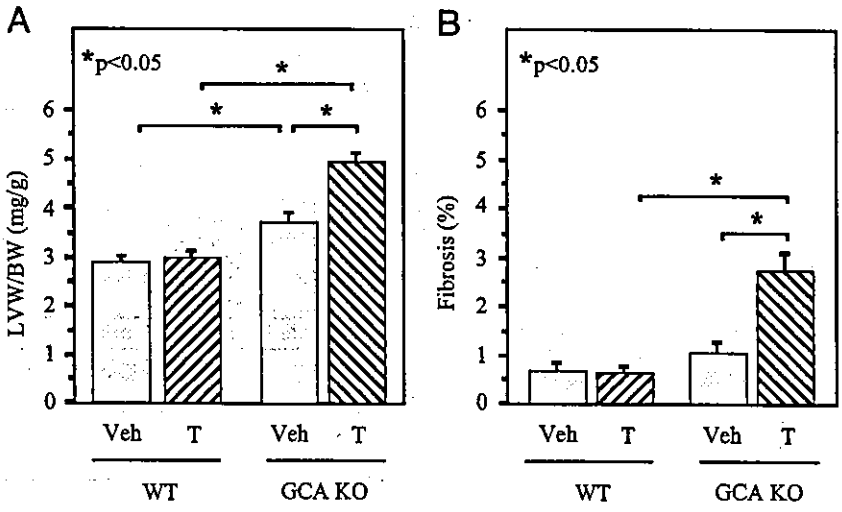

FIG. 3. Chronic infusion of testosterone (T) was associated with an increased LVW/BW (A) and left ventricular fibrosis (B) in OVX GC-A KO but not in OVX WT mice. A testosterone pellet (25.0 mg/pellet) or vehicle (Veh) was implanted sc at 10 wk of age, and 6 wk later, the animals were killed and analyses performed. Values are mean ± SEM; n = 6–7 per group; *, $P < 0.05$.

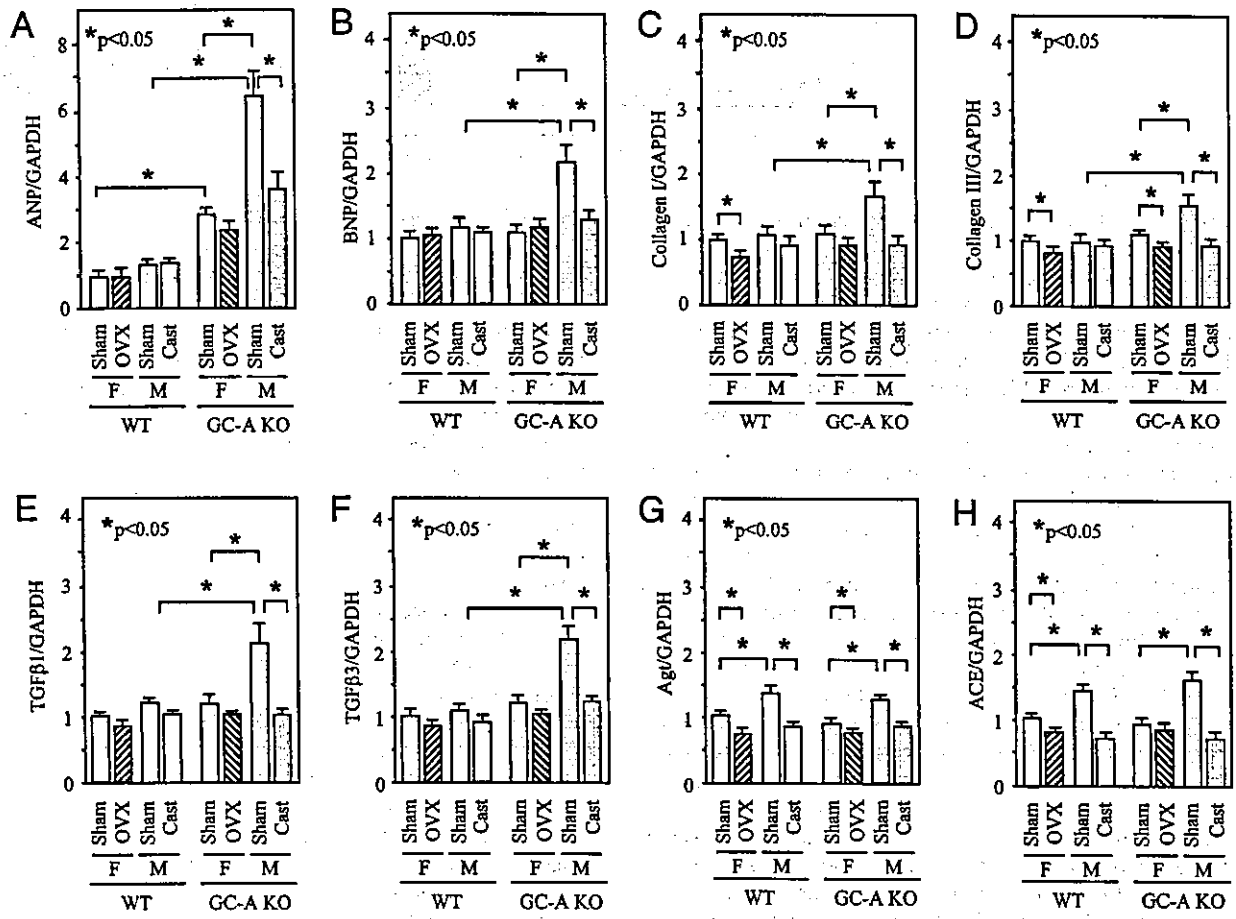

FIG. 4. Left ventricular levels of ANP, BNP, collagen I, collagen III, TGF-β1, and TGF-β3 mRNAs were elevated in male (M) GC-A KO mice and were reduced by castration to levels seen in females (F). Enhanced levels of Agt and ACE expression in male WT and GC-A KO mice were suppressed by castration, and levels were comparable in both genotypes. mRNAs were evaluated using quantitative RT-PCR in a 7700 sequence detector (ABI PRISM). Levels in sham female WT mice were arbitrarily assigned a value of 1.0. A, ANP; B, BNP; C, collagen I; D, collagen III; E, TGF-β1; F, TGF-β3; G, Agt; H, ACE. Values are mean ± SEM; n = 7–9; *, $P < 0.05$.

testosterone infusion increased cardiac mass and fibrosis only in OVX GC-A KO mice. ANP and BNP are well established molecular markers for cardiac hypertrophy. It has been demonstrated that the testosterone metabolite dihydrotestosterone is able to increase ANP secretion from ventricular myocytes. An AR antagonist, cyproterone, abolished

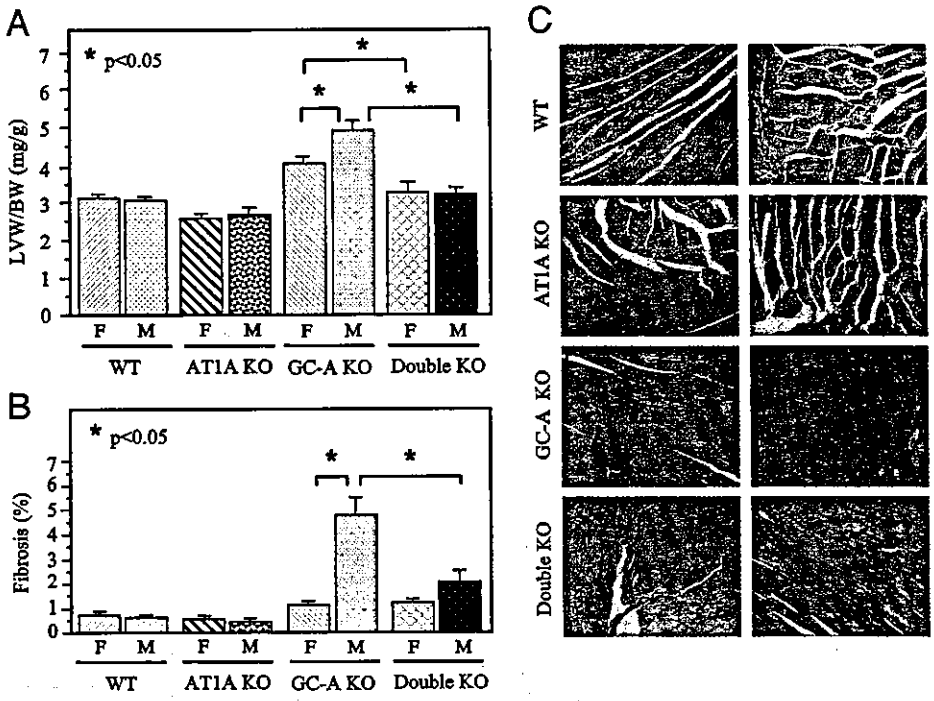

FIG. 5. Deletion of the AT1A receptor gene abolishes the gender-related differences in LVW/BW (A) and the relative levels of left ventricular fibrosis (B). C, Representative photomicrographs demonstrating fibrosis (red) in GC-A KO mice. Animals were analyzed at 16 wk of age. Values are mean ± SEM; n = 5–9 per group; *, $P < 0.05$.

this effect (12). Like cardiac geometric changes, changes in ANP and BNP, or markers for ventricular fibrosis, collagen I, and collagen III were higher in male GC-A KO mice than in females and were reduced by removal of testes. These findings suggest that androgens play an important role in gender-related cardiac differences in GC-A KO mice. Castration in males and AR antagonist could not reduce the cardiac mass and fibrosis to WT levels, suggesting that more than androgens are involved.

Ang II is known to potently stimulate cardiomyocyte and fibroblast growth, both *in vitro* and *in vivo* (31, 32), and the tissue renin-Ang system is known to play a key role in cardiac remodeling (33). It has been proposed that increased ACE abundance in the hypertrophied and failing heart may contribute to the local generation of Ang II and impact cardiac remodeling through local paracrine or autocrine effects (34–36). The greater abundance of ventricular ACE in males may contribute to the tendency of male rodents to develop cardiac abnormalities, which has been described in transgenic mouse models (37, 38) and spontaneously hypertensive rats (39) and in response to left ventricular pressure overload in rats (10) and in humans (40–42). It has been reported that hepatic Agt mRNA levels are higher in intact male hypertensive rats than in the females; moreover, those levels are reduced by orchidectomy and increased by administration of testosterone (43). Recently, Freshour *et al.* (44) demonstrated a gender difference in the expression of ACE in the murine heart with greater cardiac ACE levels seen in male animals compared with females. Moreover, ventricular ACE levels were substantially decreased in androgen-deprived males (44). Consistent with those reports, our data show that levels of cardiac Agt and ACE expression are higher in the ventricles of both GC-A KO and WT males than they are in females. Castration reduced expression of Agt in the male ventricle to levels approximating those seen in the females in both WT and GC-A KO mice. Given the evidence that Ang II has hypertrophic and fibrogenic activities in the heart, Ang II is a possible candidate to link androgens with cardiac abnormalities. It should be noted, however, that gender-related increases in LVW/BW ratios and interstitial fibrosis were observed only in the GC-A KO mice but not in WT mice, despite the similar up-regulation of Agt and ACE expression in ventricles of both genotypes of mice. We recently observed that GC-A signaling counteracts Ang II-induced cardiac abnormalities. A subpressor dose of Ang II increased cardiac mass and fibrosis only in male GC-A KO but not WT mice, suggesting an augmented responsiveness to Ang II in the heart of GC-A KO mice (22). Thus, we speculate that gender-related differences in the heart were made manifest by lacking inhibitory actions of GC-A on AT1 signaling in GC-A KO mice. Inhibitory effects of GC-A were also supported by the overexpression of TGF-β1 and -β3, which are activated by AT1A signaling and responsible for interstitial fibrosis (28, 45–47), in GC-A KO mice.

To further test this hypothesis, we deleted the AT1A receptor gene, which mediates classical Ang II actions, including cardiac hypertrophy and fibrosis, by crossing GC-A KO mice and AT1A KO mice. The gender-related cardiac differences were absent in the double-KO mice. Furthermore, castration of males did not reduce and testosterone administration failed to increase the cardiac mass and fibrosis in male double-KO mice. These results strongly suggest that GC-A prevents androgen-induced cardiac abnormalities mainly by inhibiting the androgen-Ang II-AT1A axis.

The present data did not indicate that androgens and Ang II solely provide a causative contribution to gender-related cardiac differences in GC-A KO mice. LVW/BW in male GC-A KO mice after castration or flutamide treatment were

comparable to that in female GC-A KO mice, but the degree of fibrosis was still higher in male GC-A KO mice after the treatments than in females, suggesting androgens mostly contribute to gender-related left ventricular hypertrophy, and at least approximately 50% to the gender-related increase in fibrosis. In the case of AT1A blockade, LVW/BW in GC-A KO mice were reduced to the level corresponding to that in WT mice, in which there was no difference in hypertrophy, and fibrosis was more intensively reduced by knocking out the AT1A receptor, compared with blockade of ARs. These findings suggest that AT1A signaling contributes not only to gender-related cardiac abnormalities but also to abnormalities specifically observed in both genders of GC-A KO mice, suggesting androgen is one of the factors up-regulating the Ang system. Additional studies are required to elucidate the entire mechanism for gender-related difference observed in GC-A KO mice, in which other molecules, such as catecholamines and endothelin, would be involved.

Another interesting finding is that castration or the treatment with androgen antagonist improved cardiac abnormalities in GC-A KO mice without significant change in SBP. As mentioned above, a subpressor dose of Ang II exaggerated hypertrophy and fibrosis in GC-A KO mice (22). It is likely, therefore, that androgen-induced Ang II is sufficient for inducing hypertrophy and fibrosis in GC-A KO mice but not to elevate BP.

The presence or absence of androgens in male GC-A KO mice showed marked effects on the expression levels of ANP. The molecular mechanism is unclear at present. In the present study, despite the similar up-regulation of Agt and ACE expression in ventricles of both male WT and GC-A KO mice, ANP was markedly increased only in male GC-A KO mice. We demonstrated a similar expression level of AT1A mRNA in males and females of both WT and GC-A KO mice (data not shown). Therefore, it seems that androgen-induced intracellular signaling at a postreceptor level for modulation of ANP gene expression is up-regulated in GC-A KO mice. Ang II is known to increase ANP expression mediated by protein kinase C or MAPK (48). Further examination is necessary to determine whether the protein kinase C or MAPK pathway is involved in the elevation of ANP by androgens.

Recently, Nakayama *et al.* (49) described a functional mutation in the 5′-flanking region of the human GC-A gene that reduces transcriptional activity by more than 70% in reporter gene assay, is present in approximately 5% of the hypertensive individuals in Japan, and is associated with cardiac hypertrophy. Evidence also suggests that GC-A receptors may be down-regulated in patients with chronic, severe heart failure (50). Indeed, there may be substantial numbers of patients whose abnormal GC-A signaling makes them susceptible to androgen-induced cardiac abnormalities. From the clinical points of view, the present study raises the possibility of the prophylactic use of Ang II receptor blocker or AR antagonist in patients with loss of functional mutations in the GC-A gene.

Taken together, our findings strongly support the hypothesis that androgen contributes to cardiac abnormalities *via* the AT1A receptor. Furthermore, this androgenic effect is normally inhibited by stimulation of GC-A by natriuretic peptides.

Acknowledgments

We thank Ms. Makoto Mukai and Ms. Itone Makino for their excellent secretarial assistance and Ms. Mika Inoue for her technical assistance. Dr. Yuhao Li is a foreign research fellow of the Japan Society for the Promotion of Science.

Received June 30, 2003. Accepted October 22, 2003.

Address all correspondence and requests for reprints to: Yoshihiko Saito, First Department of Internal Medicine, Nara Medical University, 840, Shijo-cho, Kashihara, Nara 634-8522, Japan. E-mail: yssaito@naramed-u.ac.jp.

This work was supported in part by research grants from Japanese Ministry of Education, Science and Culture, the Japanese Ministry of Health and Welfare, the Japanese Society for the Promotion of Science Research for the Future program (JSPS-RFTF96I00204 and JSPS-RFTF98L00801), the Uehara Memorial Foundation, the Smoking Research Foundation, and the Howard Hughes Medical Institute.

References

1. **Devereux RB, Pickering TG, Alderman MH, Chien S, Borer JS, Laragh JH** 1987 Left ventricular hypertrophy in hypertension: prevalence and relationship to pathophysiologic variables. Hypertension 9(Suppl II):53–60
2. **Kaplinsky E** 1994 Significance of left ventricular hypertrophy in cardiovascular morbidity and mortality. Cardiovasc Drugs Ther 8:549–556
3. **Neyses L, Pelzer T** 1995 The biological cascade leading to cardiac hypertrophy. Eur Heart J 16(Suppl N):8–11
4. **Weber KT, Brilla CG** 1991 Pathological hypertrophy and cardiac interstitium. Fibrosis and renin-angiotensin-aldosterone system. Circulation 83:1849–1865
5. **Hayward CS, Kelly RP, Collins P** 2000 The roles of gender, the menopause and hormone replacement on cardiovascular function. Cardiovasc Res 46: 28–49
6. **Fiebach NH, Viscoli CM, Horwitz RI** 1990 Differences between women and men in survival after myocardial infarction. JAMA 263:1092–1096
7. **de Simone G, Devereux RB, Daniels SR, Meyer RA** 1995 Gender differences in ventricular growth. Hypertension 26:979–983
8. **Luchner A, Brockel U, Muscholl M, Hense HW, Doring A, Riegger GA, Schunkert H** 2002 Gender-specific differences of cardiac remodeling in subjects with left ventricular dysfunction: a population-based study. Cardiovasc Res 53:720–727
9. **Crabbe DL, Dipla K, Ambati S, Zafeiridis A, Gaughan JP, Houser SR, Margulies KB** 2003 Gender differences in post-infarction hypertrophy in end-stage failing hearts. J Am Coll Cardiol 41:300–306
10. **Weinberg EO, Thienelt CD, Katz SE, Bartunek J, Tajima M, Rohrbach S, Douglas PS, Lorell BH** 1999 Gender differences in molecular remodeling in pressure overload hypertrophy. J Am Coll Cardiol 34:264–273
11. **Meyer R, Linz KW, Surges R, Meinardus S, Vees J, Hoffmann A, Windholz O, Grohe C** 1998 Rapid modulation of L-type calcium current by acutely applied oestrogens in isolated cardiac myocytes from human, guinea-pig and rat. Exp Physiol 83:305–321
12. **Marsh JD, Lehmann MH, Ritchie RH, Gwathmey JK, Green GE, Schiebinger RJ** 1998 Androgen receptors mediate hypertrophy in cardiac myocytes. Circulation 98:256–261
13. **Dubey RK, Gillespie DC, Jackson EK, Keller PJ** 1998 17β-Estradiol, its metabolites, and progesterone inhibit cardiac fibroblast growth. Hypertension 31:522–528
14. **Chen SJ, Li H, Durand J, Oparil S, Chen YF** 1996 estrogen reduces myointimal proliferation after balloon injury of rat carotid artery. Circulation 93:577–584
15. **Somjen D, Kohen F, Jaffe A, Amir-Zaltsman Y, Knoll E, Stern N** 1998 Effect of gonadal steroids and their antagonists on DNA synthesis in human vascular cells. Hypertension 32:39–45
16. **Fujimoto R, Morimoto I, Morita E, Sugimoto H, Ito Y, Eto S** 1994 Androgen receptors, 5α-reductase activity and androgen-dependent proliferation of vascular smooth muscle cells. J Steroid Biochem Mol Biol 50:169–174
17. **Cabral AM, Vasquez EC, Moyses MR, Antonio A** 1988 Sex hormone modulation of ventricular hypertrophy in sinoaortic denervated rats. Hypertension 11:193–197
18. **Malhotra A, Buttrick P, Scheuer J** 1990 Effects of sex hormones on development of physiological and pathological cardiac hypertrophy in male and female rats. Am J Physiol 259:H866–H871
19. **Lopez MJ, Wong SK, Kishimoto I, Dubois S, Mach V, Friesen J, Garbers DL, Beuve A** 1995 Salt-resistant hypertension in mice lacking the guanylyl cyclase-A receptor for atrial natriuretic peptide. Nature 378:65–68
20. **Oliver PM, Fox JE, Kim R, Rockman HA, Kim HS, Reddick RL, Pandey KN, Milgram SL, Smithies O, Maeda N** 1997 Hypertension, cardiac hypertrophy, and sudden death in mice lacking natriuretic peptide receptor A. Proc Natl Acad Sci USA 94:14731–14735
21. **Sugaya T, Nishimatsu S, Tanimoto K, Takimoto E, Yamagishi T, Imamura K, Goto S, Imaizumi K, Hisada Y, Otsuka A, Uchida H, Sugiura M, Fukuta**

K, Fukamizu A, Murakami K 1995 Angiotensin II type 1a receptor-deficient mice with hypotension and hyperreninemia. J Biol Chem 270:18719–18722
22. Li Y, Kishimoto I, Saito Y, Harada M, Kuwahara K, Izumi T, Takahashi N, Kawakami R, Tanimoto K, Nakagawa Y, Nakanishi M, Adachi Y, Garbers DL, Fukamizu A, Nakao K 2002 Guanylyl cyclase-A inhibits angiotensin II type 1A receptor-mediated cardiac remodeling, an endogenous protective mechanism in the heart. Circulation 106:1722–1728
23. Labrie F 1993 Mechanisms of action and pure antiandrogenic properties of flutamide. Cancer 72:3816–3827
24. Reckelhoff JF, Zhang H, Srivastava K, Granger JP 1999 Gender differences in hypertension in spontaneously hypertensive rats: role of androgens and androgen receptor. Hypertension 34:920–923
25. Mendelsohn ME, Karas RH 1999 The protective effects of estrogen on the cardiovascular system. N Engl J Med 340:1801–1811
26. van Eickels M, Grohe C, Cleutjens JP, Janssen BJ, Wellens HJ, Doevendans PA 2001 17β-Estradiol attenuates the development of pressure-overload hypertrophy. Circulation 104:1419–1423
27. Farnsworth NR, Bingel AS, Cordell GA, Crane FA, Fong HHS 1975 Potential value of plants as sources of new antifertility agents. J Pharm Sci 64:717–754
28. Price KR, Fenwick GR 1985 Naturally occurring oestrogens in foods: a review. Food Addit Contam 2:73–106
29. Degen GH, Janning P, Diel P, Bolt HM 2002 Estrogenic isoflavones in rodent diets. Toxicol Lett 128:145–157
30. Mcgill HC, Sheridan PJ 1981 Nuclear uptake of sex steroid hormones in the cardiovascular system of the baboon. Circ Res 48:238–244
31. Sadoshima J, Izumo S 1993 Molecular characterization of angiotensin II-induced hypertrophy of cardiac myocytes and hyperplasia of cardiac fibroblasts. Critical role of AT1 receptor subtype. Circ Res 73:413–423
32. Schorb W, Booz GW, Dostal DE, Conrad KM, Chang KC, Baker KM 1993 Angiotensin II is mitogenic in neonatal rat cardiac fibroblasts. Circ Res 72: 1245–1254
33. McDonald KM, Garr M, Carlyle PF, Francis GS, Hauer K, Hunter DW, Parish T, Stillman A, Cohn JN 1999 Relative effects of α1-adrenergic blockade, converting enzyme inhibitor therapy, and angiotensin II subtype 1 receptor blockade on ventricular remodeling in the dog. Circulation 90:3034–3046
34. Bader M, Peters J, Baltatu O, Muller DN, Luft FC, Ganten D 2001 Tissue rennin-angiotensin systems: new insights from experimental animal models in hypertensive research. J Mol Med 79:76–102
35. Pratt RE 1999 Angiotensin II and the control of cardiovascular structure. J Am Soc Nephrol 10:S120–S128
36. Weber KT 1997 Extra cellular matrix remodeling in heart failure. A role for de novo angiotensin II generation. Circulation 96:4065–4082
37. Kadokami T, McTieman CF, Kubota T, Frye CS, Feldman AM 2000 Sex-related survival differences in murine cardiomyopathy are associated with differences in TNF-receptor expression. J Clin Invest 106:589–597
38. Vikstrom KL, Factor SM, Leinwand LA 1996 Mice expressing mutant myosin are a model for hypertrophic cardiomyopathy. Mol Med 2:556–567
39. Wallen WJ, Cserti C, Belanger MP, Wittnich C 2000 Gender-differences in myocardial adaptation to afterload in normotensive and hypertensive rats. Hypertension 36:774–779
40. Carroll JD, Carroll EP, Feldman T, Ward DM, Lang RM, McGaughey D, Karp RB 1992 Sex-associated differences in left ventricular function in aortic stenosis of the elderly. Circulation 86:1099–1107
41. Douglas PS, Katz SE, Weinberg EO, Chen MH, Bishop SP, Lorell BH 1998 Hypertrophic remodeling: gender differences in the early response to left ventricular pressure overload. J Am Coll Cardiol 32:1118–1125
42. Villarreal FJ, Dillmann WH 1992 Cardiac hypertrophy-induced changes in mRNA levels for TGF-β1, fibronectin, and collagen. Am J Physiol Heart Circ Physiol 262:H1861–H1866
43. Chen YF, Naftilan AJ, Oparil S 1992 Androgen-dependent angiotensinogen and renin messenger RNA expression in hypertensive rats. Hypertension 19:456–463
44. Freshour JR, Chase SE, Vikstrom KL 2002 Gender differences in cardiac ACE expression are normalized in androgen-deprived male mice. Am J Physiol Heart Circ Physiol 283:H1997–H2003
45. Border WA, Nobel NA 1994 Transforming growth factor-β in tissue fibrosis. N Engl J Med 331:1286–1292
46. Kagami S, Border WA, Miller DE, Noble NA 1994 Angiotensin II stimulates extracellular matrix protein synthesis through induction of transforming growth factor-β expression in rat glomerular mesangial cells. J Clin Invest 93:2431–2437
47. Johnston CI, Hodsman PG, Kohzuki M, Casley DJ, Fabris B, Phillips PA 1989 Interaction between atrial natriuretic peptide and the renin angiotensin aldosterone system. Am J Med 87:24S–28S
48. Sadoshima J, Izumo S 1997 The cellular and molecular response of cardiac myocytes to mechanical stress. Annu Rev Physiol 59:551–571
49. Nakayama T, Soma M, Takahashi Y, Rehemudula D, Kanmatsuse K, Furuya K 2000 Functional deletion mutation of the 5′-flanking region of type A human natriuretic peptide receptor gene and its association with essential hypertension and left ventricular hypertrophy in the Japanese. Circ Res 86:841–845
50. Tsutamoto T, Kanamori T, Morigami N, Sugimoto Y, Yamaoka O, Kinoshita M 1993 Possibility of down-regulation of atrial natriuretic peptide receptor coupled to guanylate cyclase in peripheral vascular beds of patients with chronic severe heart failure. Circulation 88:811–813

Endocrinology is published monthly by The Endocrine Society (http://www.endo-society.org), the foremost professional society serving the endocrine community.

Available online at www.sciencedirect.com

SCIENCE DIRECT

Regulatory Peptides 128 (2005) 7–13

REGULATORY PEPTIDES

www.elsevier.com/locate/regpep

Chronic administration of adrenomedullin attenuates the hypertension and increases renal nitric oxide synthase in Dahl salt-sensitive rats

Fumiki Yoshihara[a,*], Shin-ichi Suga[b], Naomi Yasui[b], Takeshi Horio[a], Takeshi Tokudome[b], Toshio Nishikimi[c], Yuhei Kawano[a], Kenji Kangawa[b]

[a]*Division of Hypertension and Nephrology, National Cardiovascular center, 5-7-1 Fujishirodai, Suita, Osaka 565-8565, Japan*
[b]*National Cardiovascular Center Research Institute, 5-7-1 Fujishirodai, Suita, Osaka 565-8565, Japan*
[c]*Department of Hypertension and Cardiorenal Medicine, Dokkyo University School of Medicine, Mibu, Tochigi 321-0293, Japan*

Received 16 June 2004; accepted 10 December 2004
Available online 27 January 2005

Abstract

Adrenomedullin reduces systemic blood pressure and increases urinary sodium excretion partly through the release of nitric oxide. We hypothesized that chronic adrenomedullin infusion ameliorates salt-sensitive hypertension and increases the expression of renal nitric oxide synthase (NOS) in Dahl salt-sensitive (DS) rats, because the reduced renal NOS expression promotes salt sensitivity. DS rats and Dahl salt-resistant (DR) rats were fed a high sodium diet (8.0% NaCl) for 3 weeks. The high sodium diet resulted in an increase in blood pressure and a reduction of urinary sodium excretion in association with increased renal adrenomedullin concentrations and decreased expression of renal neuronal NOS (nNOS) and renal medullary endothelial NOS (eNOS) in DS rats compared with DR rats. Chronic adrenomedullin infusion partly inhibited the increase of blood pressure and proteinuria in association with a restoration of renal nNOS and medullary eNOS expression in DS rats under the high sodium diet. The immunohistochemical analysis revealed that the restored renal nNOS expression induced by chronic adrenomedullin infusion may reflect the restoration of nNOS expression in the macula densa and inner medullary collecting duct. These results suggest that adrenomedullin infusion has beneficial effects on this hypertension probably in part through restored renal NOS expression in DS rats.

Keywords: Adrenomedullin; Kidney; Nitric oxide synthase; Rats; Dahl; Western blot

1. Introduction

Salt sensitivity has been reported to be an independent cardiovascular risk factor in patients with hypertension [1], suggesting that the investigation of renal mechanisms of salt sensitivity is necessary to open up a possible new therapeutic strategy for hypertension. Nitric oxide (NO) was reported to stimulate an adaptive response to increased dietary sodium intake, cause vasodilation, and facilitate natriuresis [2]. The inhibition of nitric oxide synthase (NOS) was found to blunt the pressure–natriuresis relationship in normotensive rats [3], suggesting that an impaired NOS may be one of the factors causing salt-sensitive hypertension [4]. Furthermore, the reduced renal neuronal NOS (nNOS) activity in rats with salt-sensitive hypertension has been reported to promote salt sensitivity [5].

Adrenomedullin is a vasodilatory peptide originally discovered in human pheochromocytoma tissue [6]. Subsequent studies demonstrated that adrenomedullin and its specific binding sites are widely distributed in the cardiovascular system, including the kidney, heart, lungs and blood vessels [6,7]. Adrenomedullin immunoreactivity exists in glomeruli, cortical distal tubules, and medullary collecting duct cells [8]. These results suggest that adrenomedullin may play a role in the regulation of renal function. Indeed, intrarenal infusion of adrenomedullin increased the renal blood flow, glomerular filtration rate, renal sodium excretion [8]. Adrenomedullin also regulates

* Corresponding author. Tel.: +81 6 6833 5012; fax: +81 6 6872 7486.
E-mail address: fyoshi@ri.ncvc.go.jp (F. Yoshihara).

0167-0115/$ - see front matter © 2005 Elsevier B.V. All rights reserved.
doi:10.1016/j.regpep.2004.12.028

the NO production. Recently, adrenomedullin has been reported to induce NO production via the Ca^{2+}/calmodulin-dependent pathway in cultured endothelial cells [9]. These results suggested that adrenomedullin may participate in the regulation of NO production through the stimulation of eNOS and nNOS which are activated by calcium and calmodulin, and renal sodium excretion in rats with salt-sensitive hypertension.

We hypothesized that renal adrenomedullin participates in the regulation of salt sensitivity by modulating renal eNOS and nNOS, and that chronic adrenomedullin infusion ameliorates salt-sensitive hypertension and increases the expression of renal nitric oxide synthase (NOS) in Dahl salt-sensitive (DS) rats.

Thus, the purposes of this study were 1) to investigate whether the renal adrenomedullin level correlates with systemic blood pressure and urinary sodium excretion, 2) to examine whether adrenomedullin supplementation improves the salt-sensitive hypertension and affects the altered renal eNOS and nNOS expression, and 3) to evaluate where nNOS exists in the kidney in DS rats.

2. Materials and methods

2.1. Experimental animals

We used 6-week-old male DS rats and Dahl salt-resistant (DR) rats (Eisai Co. Ltd. Tokyo, Japan) in the present study. This study was performed in accordance with the guidelines of the Animal Care Committee of the National Cardiovascular Center Research Institute.

2.2. Protocol 1

The total experimental period was 4 weeks. The animals (DR rats: n=22, DS rats: n=23) were fed a regular sodium diet (0.5% NaCl) for 1 week followed by a high sodium diet (8.0% NaCl) for 3 weeks during our experimental protocol. The rats were sacrificed and the kidneys were excised for the analyses at the end of the 2nd-, 3rd-, and 4th-week of the study.

2.2.1. Urinary parameters

Twenty-four-hour urinary samples were collected from rats in metabolic cages at the end of the 1st-, 2nd-, 3rd-, and 4th-week of the study for the measurement of urinary volume and sodium excretion level. The urinary sodium level was measured by an auto-analyzer.

2.2.2. Blood pressure measurements

Systolic blood pressure was measured in conscious, restrained rats before the day of the urinary collection in every week by the tail cuff method with automated sphygmomanometers. Rats were placed in individual restrainers and pre-warmed at 37 °C. The average of three readings was recorded.

2.2.3. Measurements of renal tissue adrenomedulln

The rat adrenomedullin levels in the renal cortex and medulla were measured at the end of the 4th-week of the study in DS and DR rats. Radioimmunoassay for rat adrenomedullin was performed as described previously [10].

2.2.4. Western blot analysis

Western blotting for eNOS and nNOS in the renal cortex and medulla (DR rats, n=4; DS rats, n=4) was carried out at the end of the 4th-week of the study [11]. Twenty-microgram kidney tissue preparations were size-fractionated on 4–12% Tris-Glycine gel (Bio-Rad) at 200V for 1.5 h. After electrophoresis, proteins were transferred onto Immobilon-P membrane (Millipore) at 350 mA for 100 min. The membrane was prehybridized in 10 mL of TBST (10 mmol/L Tris hydrochloride, pH 7.5, 100 mmol/L NaCl, 0.1% Tween 20) containing 5% nonfat milk for 2 h and hybridized overnight in the same buffer containing anti-eNOS or anti-nNOS monoclonal antibodies (1:750, Transduction Labs). The membrane was then washed for 30 min with TBST and then incubated with TBST with 5% nonfat milk and goat anti-mouse IgG-horseradish peroxidase (1:1000, Amersham) After the washes, the membrane was developed with a chemiluminating method using ECL reagent (Amersham Inc). The membrane was then subjected to autoluminography for 5–10 min. The autoluminographs were scanned with a laser densitometer to determine the relative optical densities of the bands. The membranes were stained with India ink before prehybridization to confirm an equal amount of protein loading and transfer efficiency among the samples.

2.3. Protocol 2

The experimental period and the feeding protocol were identical to those of protocol 1. Before the 2nd-week, DS rats were randomly divided into 2 groups; the adrenomedullin-treated group and the untreated group. After pentobarbital sodium anesthesia (30 mg/kg, IP), the rats were subcutaneously implanted with an osmotic minipump (Model 2ML4, Alza) filled with recombinant human adrenomedullin dissolved in 0.9% saline in the adrenomedullin-treated group (DS-AM, 400 ng/hr per rat, n=14) and and 0.9% saline in the untreated group (DS-S, n=14). for evaluating the effects of adrenomedullin infusion on systolic blood pressure and urinary sodium excretion under the high sodium diet.

2.3.1. Recombinant human adrenomedullin

Recombinant human adrenomedullin was kindly provided by Shionogi Pharmaceutical, Osaka, Japan. Adrenomedullin with a glycine extension residue at the C-terminus (adrenomedullin-gly) was expressed in *Escherichia coli*. The product was digested with a site-specific protease after denaturation. The resulting adrenomedullin-gly was amidated by a peptidyl-glycine amidating enzyme for conversion to the mature form of adrenomedullin with an amidated C-terminus.

2.3.2. Urinary parameters, blood pressure measurements, and western blot analysis

Twenty-four-hour urinary samples were collected from rats in metabolic cages at the end of each week throughout the study for the measurement of urinary volume and protein excretion. Urinary sodium excretion was measured at the end of 4th-week. Systolic blood pressure was measured before the day of the urine collection. Western blot analysis for eNOS and nNOS in the renal cortex and medulla was performed at the end of protocol 2.

2.3.3. Immunohistochemistry

For immunohistochemical analysis, the kidneys were fixed with Methyl Carnoy. The tissues were embedded in paraffin, and 3-μm-thick sections were cut and mounted on glass slides treated with silica. An indirect immunoperoxidase method was used to identify the nNOS antigen (a mouse IgG to neuronal NOS, Transduction Labs) [12].

2.4. Statistical analysis

All values are presented as mean±SD. Comparisons of 3 or more groups were performed by ANOVA with the Scheffe's post hoc test. Comparisons between 2 groups were performed by the unpaired t test. Differences were considered statistically significant at a level of $p<0.05$. Correlation coefficients were calculated using linear regression analysis.

3. Results

3.1. Protocol 1

Body weight was significantly reduced and left ventricular plus septal weight was significantly increased at the 4th-week in DS rats compared with DR rats (Table 1). Kidney weight was also increased after the 3rd-week in DS rats compared with DR rats (Table 1). Systolic blood pressure and urinary sodium excretion were not significantly different between DS and DR rats at the 2nd-week (Table 1). While systolic blood pressure significantly increased after the 3rd-week, urinary sodium excretion decreased only at the 4th-week in DS rats compared with DR rats (Table 1).

Table 2
Correlations between renal adrenomedullin (AM) concentrations with urinary sodium excretion and systolic blood pressure at the 4th-week in protocol 1

	Cortical AM (fmol/mg)	Medullary AM (fmol/mg)
Urinary Na excretion (mmol/day)	$R=-0.68$, $p<0.01$	$R=-0.60$, $p<0.05$
Systolic Blood Pressure (mmHg)	$R=0.85$, $p<0.0001$	$R=0.86$, $p<0.0001$

The tissue adrenomedullin concentrations in both the renal cortex and medulla were significantly increased at the end of 4th-week in DS rats compared with DR rats (Table 1). The increased renal adrenomedullin levels in the renal cortex and medulla inversely correlated with urinary sodium excretion and positively correlated with systolic blood pressure (Table 2). Western blot analysis revealed that the eNOS expression in the renal medulla and the nNOS expression in both the renal cortex and medulla were significantly lower in DS rats compared with DR rats at the end of the 4th-week (Fig. 1). However, renal cortical eNOS expression was comparable between DS and DR rats (Fig. 1).

3.2. Protocol 2

The chronic adrenomedullin infusion did not affect body and kidney weight in DS rats, however, its infusion significantly reduced the left ventricular and septal weight in DS rats at the end of the 4th-week (Table 3). The chronic adrenomedullin infusion significantly reduced systolic blood pressure and tended to increase urinary sodium excretion at the 4th-week in DS rats under the high sodium diet (Table 3). Chronic adrenomedullin infusion signifi-

Table 1
Number, body weight, heart rate, heart and kidney weights in Dahl rats during feeding on the high sodium diet

	2nd-week		3rd-week		4th-week	
	DR	DS	DR	DS	DR	DS
N	7	8	8	7	7	8
BW (g)	286±16	292±9	309±11	297±14	371±12	342±12**
HR (bpm)	389±24	398±37	396±36	373±10	377±22	399±25
LV+SEP/BW (mg/g)	2.06±0.15	2.19±0.07	2.22±0.16	2.42±0.07	1.97±0.11	2.58±0.13#
Kid/BW (mg/g)	3.69±0.26	3.91±0.14	4.09±0.13	4.46±0.20*	3.67±0.13	4.64±0.19#
SBP (mmHg)	119±8	126±6	124±9	166±5#	125±8	169±7#
UNaV (mmol/day)	2.1±1.0	2.4±0.7	1.9±0.6	1.9±0.9	2.7±1.3	1.2±0.3**
Cortical AM (fmol/mg)	0.59±0.10	0.62±0.05	0.56±0.06	0.61±0.09	0.55±0.06	0.74±0.06**
Medullary AM (fmol/mg)	0.31±0.06	0.31±0.05	0.34±0.04	0.31±0.05	0.34±0.02	0.45±0.04**

N indicates number of rats; BW, body weight; HR, heart rate; LV+SEP, left ventricular and septal weight; Kid, kidney weight; SBP, systolic blood pressure; UNaV, urinary sodium excretion. Data are mean±SD.

# $p<0.0001$ vs DR at the same period, * $p<0.05$ vs DR, ** $p<0.01$ vs DR.

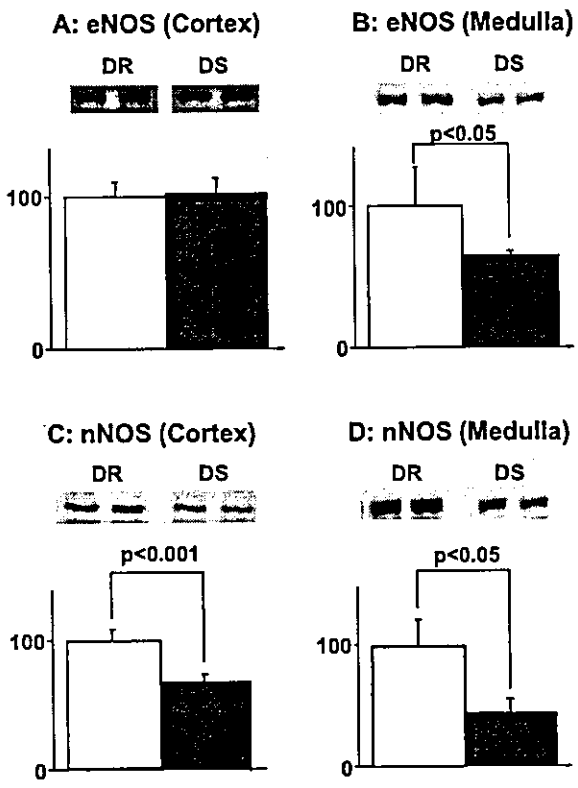

Fig. 1. Representative Western blots showing NOS and relative abundance of NOS in the renal cortex and medulla at the end of the 4th-week in Dahl rats in protocol 1 (n=4, in each group). A, B: eNOS; C,D: nNOS.

cantly restored eNOS expression in the renal medulla and nNOS expression in the renal cortex and medulla in DS rats at the end of the 4th-week (Fig. 2). Furthermore, the levels of proteinuria were significantly higher in DS rats than DR rats during all over the high sodium diet and chronic adrenomedullin infusion significantly inhibited the increasing of proteinuria levels under the high sodium diet in DS rats (Table 4). The immunohistochemical analysis revealed

Table 3
Number, body weight, heart rate, heart and kidney weights in Dahl rats treated with saline or adrenomedullin at the end of the 4th-week

	DR-S	DS-S	DS-AM
N	19	14	14
BW (g)	370±11	348±15*	350±14*
HR (bpm)	347±32	355±38	332±35
LV+SEP/BW (mg/g)	1.90±0.13	2.54±0.13*	2.32±0.14[a,*]
Kid/BW (mg/g)	3.85±0.28	4.63±0.26*	4.52±0.27*
SBP (mmHg)	128±6	173±10**	150±10[b,**]
UNaV (mmol/day)	2.2±0.7	1.4±0.5*	1.7±0.5

Abbreviations as in Table 1. DR-S indicates DR rats treated with saline; DS-S, DS rats treated with saline; DS-AM, DS rats treated with adrenomedullin. Data are mean±SD.

[a] p<0.001 vs DS-S.
[b] p<0.001 vs DS-S.
* p<0.001 vs DR-S.
** p<0.0001 vs DR-S.

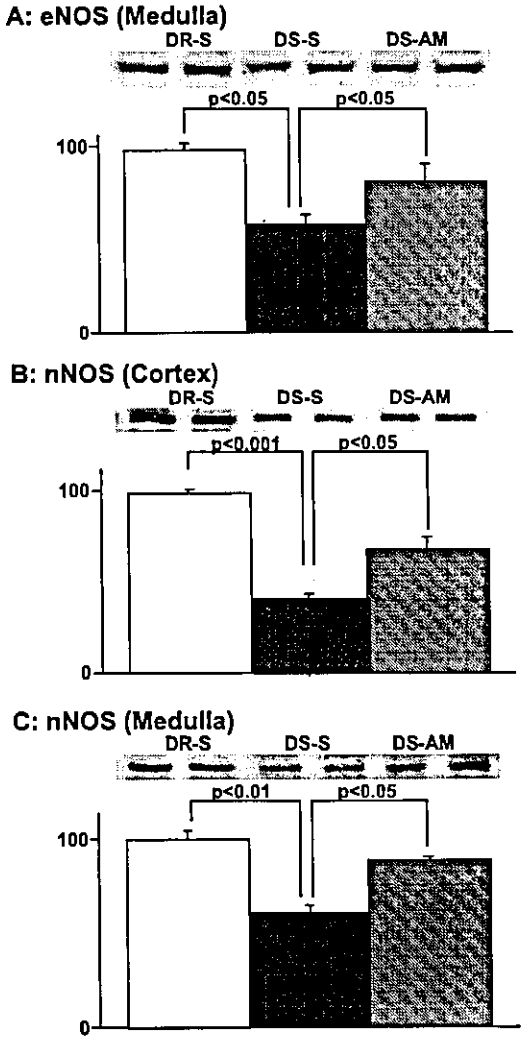

Fig. 2. The effect of chronic adrenomedullin infusion on the NOS expression in the renal cortex and medulla at the end of the 4th-week in protocol 2 (n=4, in each group). A: eNOS; B,C: nNOS.

that nNOS was localized in the macula densa and inner medullary collecting duct cells in all groups (Fig. 3).

4. Discussion

In the present study, we demonstrated for the first time that 1) the tissue adrenomedullin levels in the renal cortex and medulla significantly increased in DS rats compared with DR rats after 3 weeks on a high sodium diet, and were negatively correlated with urinary sodium excretion and positively correlated with systolic blood pressure, 2) the expression of eNOS in the renal medulla and nNOS in the renal cortex and medulla significantly reduced in DS rats, 3) chronic adrenomedullin supplementation significantly reduced systolic blood pressure, tended to increase urinary sodium excretion, and reduced urinary protein excretion in association with the restoration of renal medullary eNOS